

Last modified: January 20, 2006

Sensitivity and Uncertainty Analysis for Eigenvalue-Difference Responses

Mark L. Williams

Oak Ridge National Laboratory*
Nuclear Science and Technology Division
P.O. Box 2008, MS-6170
Oak Ridge, TN 37831-6170 USA
Telephone: (865) 576-5565
Fax: (865) 576-3513
E-mail: williamsml@ornl.gov

For submission to
Nuclear Science and Engineering

Total number of pages: 59
Total number of figures: 7
Total number of tables: 6

The submitted manuscript has been authored by a contractor of the U.S. Government under contract No. DE-AC05-00OR22725. Accordingly, the U.S. Government retains a nonexclusive, royalty-free license to publish or reproduce the published form of this contribution, or allow others to do so, for U.S. Government purposes.

* Managed by UT-Battelle, LLC, under contract DE-AC05-00OR22725 with the U.S. Department of Energy.

Sensitivity and Uncertainty Analysis for Eigenvalue-Difference Responses

Mark L. Williams

Oak Ridge National Laboratory[†]
Nuclear Science and Technology Division
P.O. Box 2008, Bldg. 5700, MS-6170
Oak Ridge, TN 37831-6170
Telephone: 865-576-5565
Fax: 865-576-3513
E-mail: williamsml@ornl.gov

Abstract

Equations for sensitivity coefficients of eigenvalue-difference responses such as reactivity are derived from a unified approach based on both eigenvalue and generalized perturbation theory. The sensitivity coefficients are utilized for uncertainty analysis of reactivity responses, and it is shown that these types of responses have inherently larger relative uncertainties than eigenvalue responses. Monte Carlo calculations are used to apply the methodology to the analysis of the coolant void reactivity in a 3D model of a fuel bundle in an advanced CANDU reactor system. The important data sensitivities are identified, and it is shown that the coolant void reactivity has a large uncertainty due to nuclear data uncertainties.

[†] Managed by UT-Battelle, LLC, under contract DE-AC05-00OR22725 with the U.S. Department of Energy.

I. INTRODUCTION

For many years techniques based on first-order perturbation theory have been developed to treat a wide range of applications in reactor analysis.¹⁻⁵ Recently, perturbation methods have been applied in the criticality safety field to assess the impact of data uncertainties on the computed sub-criticality margin and to quantify the similarity of calculated sub-critical configurations to the critical benchmark experiments used in validating the computational methods.⁶⁻⁷ In this work we describe the use of perturbation theory for sensitivity and uncertainty (S/U) analysis of a response corresponding to the difference in critical eigenvalues for two distinct systems. The most obvious application for this method is in determining the data sensitivities and uncertainties of reactivity responses such as control rod worths, fuel and moderator temperature coefficients, and void coefficients in a power reactor at two defined conditions. However, another potential application is in the analysis of benchmark criticals for nuclear data testing and for establishing computational biases. Nuclear data and methods validation is often performed by calculating a series of similar benchmark experiments that differ in only a few parameters such as critical boron concentration, fuel enrichment, etc. Data deficiencies can introduce a computational bias manifested as a trend in calculated/measured eigenvalues versus experiment parameters. The S/U methods described here can be applied directly to the *difference* in the computed eigenvalues of two benchmarks to establish the sensitivity of the bias to various nuclear data used in the calculations. This procedure may provide insight for improved data evaluation, as well as a better understanding of the sources of computational biases.

In this paper, the difference in lambda eigenvalues is called the “reactivity” associated with two “states,” even though the states may actually correspond to different critical systems, as in the case of two benchmark experiments. Simple eigenvalue perturbation theory can be used to derive sensitivity coefficients for the eigenvalue-difference of the two distinct states. This approach for addressing reactivity responses is attractive because the SCALE code system, developed by Oak Ridge National Laboratory (ORNL), includes automated calculation sequences for eigenvalue S/U analysis.⁸ The sequence called TSUNAMI-1D⁹ uses one-dimensional (1D) discrete ordinates, while TSUNAMI-3D¹⁰ uses Monte Carlo to calculate eigenvalue sensitivities in arbitrary 3D geometry. Both code sequences include techniques to account for perturbations in cross-section self-shielding.¹¹

An alternative formulation based on “exact perturbation theory” represents the reactivity response as a bilinear functional ratio.¹² During the 1960s and 1970s, generalized perturbation theory (GPT) was developed to address these types of responses,¹³ as discussed in detail by Stacy.¹⁴ The GPT method involves solving inhomogeneous “generalized adjoint” and “generalized forward” transport equations. Gandini has also described a method called “equivalent generalized perturbation theory (EGPT),” in which the generalized forward and adjoint solutions are replaced by solutions of homogeneous equations.¹⁵ In the case of reactivity responses, this approach is equivalent to simply applying eigenvalue perturbation theory at the two states, as done in this work.

In section II of this paper, it is shown that a unified approach can be used to derive sensitivity coefficient expressions for the two different formulations of the

eigenvalue-difference response, which leads to two different types of reactivity sensitivity coefficients — one based on eigenvalue perturbation theory and the other on GPT. Section III examines how eigenvalue-difference sensitivities are used to compute the uncertainty in a reactivity response due to nuclear data uncertainties. It is shown that a covariance term is present as a result of correlations in the two states, and that reactivity responses inherently have higher relative uncertainties than the eigenvalue uncertainties for the two states. In section IV, eigenvalue-difference sensitivity coefficients computed by perturbation theory are compared with “direct” results based on finite difference calculations for a 1D model of a light water reactor (LWR) pincell. Finally, Monte Carlo calculations are used to obtain sensitivity coefficients for the coolant-voiding reactivity in a 3D model of a fuel bundle in the advanced CANDU reactor, ACR-700. A comparison of the sensitivity coefficients shows that the reactivity response can be much more sensitive to data uncertainties than the eigenvalues for the two states. This leads to a significantly higher uncertainty in the calculated reactivity.

II. REACTIVITY EXPRESSIONS

It is assumed that a reactor system is initially in some well defined state 1 having a lambda-mode eigenvalue of λ_1 , where the lambda eigenvalue is defined as the reciprocal of the multiplication factor; i.e., $\lambda_1 = \frac{1}{k_1}$. The neutron flux in state 1 of this system is represented by the fundamental solution to the forward lambda mode eigenvalue equation

$$(\mathbf{L}_1 - \lambda_1 \mathbf{P}_1)\Phi_1 = 0 \quad , \quad (1)$$

where \mathbf{L}_1 and \mathbf{P}_1 are the production and loss operators for state 1. The static reactivity ρ for state 1 is defined as $\rho_1 = 1 - \lambda_1$.

Suppose that the following arbitrary modifications are made in the system

$$\mathbf{L}_1 \rightarrow \mathbf{L}_2 = \mathbf{L}_1 + \Delta\mathbf{L} \quad ; \quad (2a)$$

$$\mathbf{P}_1 \rightarrow \mathbf{P}_2 = \mathbf{P}_1 + \Delta\mathbf{P} \quad . \quad (2b)$$

The system modifications have no restrictions. For example, these could correspond to changes in fuel loading, complete voiding of the coolant density, or the temperature difference between cold and hot core conditions. The modifications transform the original system to a new distinct configuration designated as state 2 with a lambda eigenvalue of

$$\lambda_2 = \lambda_1 + \Delta\lambda_{1 \rightarrow 2} \quad (3)$$

and static reactivity of $\rho_2 = 1 - \lambda_2$. The perturbed system has an altered flux distribution given by the solution of the eigenvalue equation,

$$(\mathbf{L}_2 - \lambda_2 \mathbf{P}_2) \Phi_2 = 0 \quad . \quad (4)$$

The adjoint equations for Eqs. (1) and (4), respectively, correspond to

$$(\mathbf{L}_1^* - \lambda_1 \mathbf{P}_1^*) \Phi_1^* = 0 \quad (5a)$$

and

$$(\mathbf{L}_2^* - \lambda_2 \mathbf{P}_2^*) \Phi_2^* = 0 \quad . \quad (5b)$$

Expressions for the two lambda eigenvalues λ_1 and λ_2 are found by taking the inner products of both sides of Eqs. (1) and (4), respectively, with the *unspecified* weight functions $\tilde{\varphi}_1^*$ and $\tilde{\varphi}_2^*$, and solving for:

$$\lambda_1 = \frac{\langle \tilde{\varphi}_1^* \mathbf{L}_1 \Phi_1 \rangle}{\langle \tilde{\varphi}_1^* \mathbf{P}_1 \Phi_1 \rangle} \quad \text{and} \quad (6a)$$

$$\lambda_2 = \frac{\langle \tilde{\varphi}_2^* \mathbf{L}_2 \Phi_2 \rangle}{\langle \tilde{\varphi}_2^* \mathbf{P}_2 \Phi_2 \rangle} . \quad (6b)$$

Equations (6a) and (6b) are bilinear ratio forms known as the Rayleigh quotient expression for the eigenvalue. It is emphasized that $\tilde{\varphi}_1^*$ and $\tilde{\varphi}_2^*$ are arbitrary, and not necessarily solutions to the adjoint equations in Eqs. (5a) and (5b). The eigenvalue expressions in Eqs. (6a) and (6b) are exact for any non-zero functions $[\tilde{\varphi}_1^*, \tilde{\varphi}_2^*]$ defined over the same domain as the solutions of Eqs. (1) and (3), as long as they do not make the denominators equal to zero (i.e., $\tilde{\varphi}_1^*$ and $\tilde{\varphi}_2^*$ cannot be orthogonal to the fission sources). Throughout this work, a tilde will continue to be used to represent arbitrary functions of this type.

Two additional eigenvalue expressions are obtained by taking the inner products of the adjoint equations in Eqs. (5a) and (5b), respectively, with two other unspecified weight functions $\tilde{\varphi}_1$ and $\tilde{\varphi}_2$, and solving for the eigenvalue:

$$\lambda_1 = \frac{\langle \tilde{\varphi}_1 \mathbf{L}_1^* \Phi_1^* \rangle}{\langle \tilde{\varphi}_1 \mathbf{P}_1^* \Phi_1^* \rangle} \quad \text{and} \quad (7a)$$

$$\lambda_2 = \frac{\langle \tilde{\varphi}_2 \mathbf{L}_2^* \Phi_2^* \rangle}{\langle \tilde{\varphi}_2 \mathbf{P}_2^* \Phi_2^* \rangle} . \quad (7b)$$

Again, the above expressions are exact for any two arbitrary functions $\tilde{\varphi}_1$ and $\tilde{\varphi}_2$ in the flux domain that are non-orthogonal to the adjoint fission sources. Equations (7a) and (7b), along with Eqs. (6a) and (6b), are bilinear functional ratio expressions for the eigenvalues. In this work, they are the basis for deriving eigenvalue and reactivity sensitivity coefficients in a consistent and unified manner.

The reactivity insertion/withdrawal associated with the designated change of state is defined as

$$\rho_{1 \rightarrow 2} = \rho_2 - \rho_1 = \lambda_1 - \lambda_2 . \quad (8)$$

In the remainder of this paper, the term “reactivity” will refer to this reactivity change, rather than the static reactivity of a fixed state. Aside from a difference in sign, the reactivity is equivalent to the lambda eigenvalue-difference. The above reactivity can be expressed in several different ways. By substituting Eqs. (6a) and (6b) into Eq. (8), it is seen that

$$\rho_{1 \rightarrow 2} = \frac{\langle \tilde{\varphi}_1^* \mathbf{L}_1 \Phi_1 \rangle}{\langle \tilde{\varphi}_1^* \mathbf{P}_1 \Phi_1 \rangle} - \frac{\langle \tilde{\varphi}_2^* \mathbf{L}_2 \Phi_2 \rangle}{\langle \tilde{\varphi}_2^* \mathbf{P}_2 \Phi_2 \rangle} . \quad (9)$$

Substituting Eqs. (7a) and (7b) into Eq. (8) would give an analogous equation in terms of the adjoint solutions. Since the weight functions $\tilde{\varphi}_1^*$ and $\tilde{\varphi}_2^*$ are arbitrary (for example, they could be defined to be unity), it is necessary only to perform two forward eigenvalue calculations—i.e., at state 1 and state 2, respectively—to compute the reactivity by evaluating the integrals in Eq. (9). Alternatively, adjoint calculations could be performed at state 1 and state 2, respectively, and Eqs. (7a) and (7b) used to compute the two ratios appearing in the reactivity expression. In either case, essentially the same amount of effort is required to evaluate the bilinear ratios as to compute the eigenvalues for the two states and subtract, as in Eq. (8).

Equation (9) can also be manipulated to give another reactivity expression known as “exact perturbation theory.” This is done as follows: substitute Eq. (2a) for \mathbf{L}_2 in the second term on the right side of Eq. (9),

$$\rho_{1 \rightarrow 2} = \frac{\langle \tilde{\varphi}_1^* \mathbf{L}_1 \Phi_1 \rangle}{\langle \tilde{\varphi}_1^* \mathbf{P}_1 \Phi_1 \rangle} - \left\{ \frac{\langle \tilde{\varphi}_2^* \mathbf{L}_1 \Phi_2 \rangle}{\langle \tilde{\varphi}_2^* \mathbf{P}_2 \Phi_2 \rangle} + \frac{\langle \tilde{\varphi}_2^* \Delta \mathbf{L} \Phi_2 \rangle}{\langle \tilde{\varphi}_2^* \mathbf{P}_2 \Phi_2 \rangle} \right\}. \quad (10)$$

The first term inside of the brackets can be rearranged as

$$\frac{\langle \tilde{\varphi}_2^* \mathbf{L}_1 \Phi_2 \rangle}{\langle \tilde{\varphi}_2^* \mathbf{P}_2 \Phi_2 \rangle} = \frac{\langle \tilde{\varphi}_2^* \mathbf{L}_1 \Phi_2 \rangle}{\langle \tilde{\varphi}_2^* \mathbf{P}_1 \Phi_2 \rangle} - \frac{\langle \tilde{\varphi}_2^* \mathbf{L}_1 \Phi_2 \rangle}{\langle \tilde{\varphi}_2^* \mathbf{P}_1 \Phi_2 \rangle} \frac{\langle \tilde{\varphi}_2^* \Delta \mathbf{P} \Phi_2 \rangle}{\langle \tilde{\varphi}_2^* \mathbf{P}_2 \Phi_2 \rangle},$$

and when this expression is substituted back into Eq. (10), we see that

$$\rho_{1 \rightarrow 2} = \frac{\langle \tilde{\varphi}_1^* \mathbf{L}_1 \Phi_1 \rangle}{\langle \tilde{\varphi}_1^* \mathbf{P}_1 \Phi_1 \rangle} - \frac{\langle \tilde{\varphi}_2^* \mathbf{L}_1 \Phi_2 \rangle}{\langle \tilde{\varphi}_2^* \mathbf{P}_1 \Phi_2 \rangle} + \frac{\langle \tilde{\varphi}_2^* \mathbf{L}_1 \Phi_2 \rangle}{\langle \tilde{\varphi}_2^* \mathbf{P}_1 \Phi_2 \rangle} \frac{\langle \tilde{\varphi}_2^* \Delta \mathbf{P} \Phi_2 \rangle}{\langle \tilde{\varphi}_2^* \mathbf{P}_2 \Phi_2 \rangle} - \frac{\langle \tilde{\varphi}_2^* \Delta \mathbf{L} \Phi_2 \rangle}{\langle \tilde{\varphi}_2^* \mathbf{P}_2 \Phi_2 \rangle}. \quad (11)$$

Equation (11) is completely general, but if the arbitrary weight function $\tilde{\varphi}_2^*$ is defined to be the particular function Φ_1^* that is the solution to Eq. (5a), then the first two terms on the right side of Eq. 11 are both equal to λ_1 . Therefore, an exact perturbation theory expression for the reactivity is

$$\rho_{1 \rightarrow 2} = \frac{\langle \Phi_1^* (\lambda_1 \Delta \mathbf{P} - \Delta \mathbf{L}) \Phi_2 \rangle}{\langle \Phi_1^* \mathbf{P}_2 \Phi_2 \rangle} = \lambda_1 \frac{\langle \Phi_1^* \Delta \mathbf{P} \Phi_2 \rangle}{\langle \Phi_1^* \mathbf{P}_2 \Phi_2 \rangle} - \lambda_2 \frac{\langle \Phi_1^* \Delta \mathbf{L} \Phi_2 \rangle}{\langle \Phi_1^* \mathbf{L}_2 \Phi_2 \rangle}. \quad (12)$$

These equations also can be derived directly from the lambda mode eigenvalue equations by applying standard perturbation theory techniques.¹⁴ Equation (12) is not limited to small perturbations in $\Delta \mathbf{L}$ and $\Delta \mathbf{P}$. Just as in Eq. (9), the evaluation of Eq. (12) again requires two eigenvalue calculations; however, in this case, the calculations correspond to a forward solution at one state and an adjoint at the other, and no arbitrary weight functions appear.

Each of the derived reactivity expressions requires two solutions of the lambda mode eigenvalue equation. The most common method to determine the reactivity associated with a known change in state has been to subtract the lambda eigenvalues computed for the two states. However, in dealing with small reactivities associated with a

well-defined change in state, it may be more accurate to use exact perturbation theory since it does not require subtracting two computed quantities with nearly the same magnitude.

III. SENSITIVITY COEFFICIENTS

The theoretical basis for sensitivity analysis of eigenvalue responses, as well as reactivity responses, is well established. Here we present a unified derivation, so that the relationship between reactivity sensitivity coefficients based on traditional eigenvalue differences and on GPT can be seen.

The computed value of a response R , such as the eigenvalue at a single state or the reactivity change between two states, depends upon the input multigroup cross sections and modeling parameters used in the calculation. In S/U analysis, it is desired to determine how much the response varies as a result of changes in the reference input parameters. The response variation is usually approximated by the first-order terms in a Taylor series expansion about the initial data α , so that the response change is proportional to the data change, and the contributions of each parameter can be computed independently and summed to obtain the total response change. The first-order

approximation relating $\frac{\Delta R}{R}$ and some data perturbation $\frac{\Delta \alpha}{\alpha}$ is given by

$$\frac{\Delta R}{R} \sim S_{R,\alpha} \frac{\Delta \alpha}{\alpha} , \quad (13)$$

where the relative sensitivity coefficient is defined as $S_{R,\alpha} \equiv \frac{\alpha}{R} \frac{\partial R}{\partial \alpha}$. In this work, we

derive theoretically exact expressions for the linear sensitivity coefficients of a reactivity

(i.e., eigenvalue-difference) response. However, even if the sensitivity coefficients, and hence the response derivatives, are known exactly, the reactivity perturbation is not computed exactly because the higher-order terms are omitted in Eq. (13). Since the reactivity depends upon eigenvalue responses in two states, it is useful first to develop eigenvalue sensitivity coefficients expressed in a manner that is readily extended to the reactivity response.

III.A. Eigenvalue Sensitivity Coefficients

The relative sensitivity coefficient for the lambda eigenvalue response is given by

$$\tilde{S}_{\lambda,\alpha} = \frac{\alpha}{\lambda} \frac{\partial \lambda}{\partial \alpha} \quad , \quad (14a)$$

and the relative sensitivity coefficient for the multiplication factor ($k=1/\lambda$) is

$$\tilde{S}_{k,\alpha} = \frac{\alpha}{k} \frac{\partial k}{\partial \alpha} = -\tilde{S}_{\lambda,\alpha} \quad . \quad (14b)$$

The tilde appearing in the sensitivity notation indicates that the most general lambda expressions given in Eqs. (6a–6b) and (7a–7b) may contain arbitrary weight functions such as $\tilde{\varphi}_1$, $\tilde{\varphi}_2$, $\tilde{\varphi}_1^*$, $\tilde{\varphi}_2^*$, etc. The eigenvalue derivatives with respect to α can be found by differentiating the Rayleigh quotients in Eqs. (6a) and (6b), for states 1 and 2 respectively. For example, the derivative of λ for state 1 is equal to

$$\frac{\partial \lambda_1}{\partial \alpha} = \lambda_1 \left\{ \frac{\left\langle \tilde{\varphi}_1^* \frac{\partial \mathbf{L}_1}{\partial \alpha} \Phi_1 \right\rangle}{\left\langle \tilde{\varphi}_1^* \mathbf{L}_1 \Phi_1 \right\rangle} - \frac{\left\langle \tilde{\varphi}_1^* \frac{\partial \mathbf{P}_1}{\partial \alpha} \Phi_1 \right\rangle}{\left\langle \tilde{\varphi}_1^* \mathbf{P}_1 \Phi_1 \right\rangle} + \frac{\left\langle \tilde{\varphi}_1^* \mathbf{L}_1 \frac{\partial \Phi_1}{\partial \alpha} \right\rangle}{\left\langle \tilde{\varphi}_1^* \mathbf{L}_1 \Phi_1 \right\rangle} - \frac{\left\langle \tilde{\varphi}_1^* \mathbf{P}_1 \frac{\partial \Phi_1}{\partial \alpha} \right\rangle}{\left\langle \tilde{\varphi}_1^* \mathbf{P}_1 \Phi_1 \right\rangle} \right\} . \quad (15)$$

Substituting the definition of λ_1 from Eq. (6a) into Eq. (15), and then multiplying by $\frac{\alpha}{\lambda_1}$, the relative sensitivity coefficient for the lambda eigenvalue of state 1 is found to be

$$\tilde{S}_{\lambda_1\alpha} = \left\{ \frac{\left\langle \tilde{\varphi}_1^* \left(\frac{\alpha \partial \mathbf{L}_1}{\partial \alpha} - \lambda_1 \frac{\alpha \partial \mathbf{P}_1}{\partial \alpha} \right) \Phi_1 \right\rangle}{\lambda_1 \langle \tilde{\varphi}_1^* \mathbf{P}_1 \Phi_1 \rangle} + \frac{\left\langle \frac{\alpha \partial \Phi_1}{\partial \alpha} (\mathbf{L}_1^* - \lambda_1 \mathbf{P}_1^*) \tilde{\varphi}_1^* \right\rangle}{\lambda_1 \langle \tilde{\varphi}_1^* \mathbf{P}_1 \Phi_1 \rangle} \right\}. \quad (16)$$

An analogous procedure is applied to Eq. (6b) to find the λ_2 sensitivity coefficient, which corresponds to Eq. (16) with subscript “1” replaced by “2.” Two more expressions for the sensitivity coefficients of λ_1 and λ_2 also can be found by differentiating Eqs. (7a) and (7b), respectively. The resulting $\tilde{S}_{\lambda_i\alpha}$ expression, for example, is similar to Eq. (16) except that the flux and the \mathbf{L} and \mathbf{P} operators are replaced by their adjoints.

The general expression for the lambda sensitivity coefficient in Eq. (16) contains one arbitrary function [$\tilde{\varphi}_1^*$] along with one function [Φ_1] obtained from an eigenvalue solution, suggesting that only a single calculation (either forward or adjoint) is required to determine the sensitivity coefficient for a given state. However, this conclusion is misleading because Eq. (16) also contains the unknown values for the flux (or adjoint) derivatives such as $\frac{\partial \Phi_1}{\partial \alpha}$, which must be found from additional calculations. Simply ignoring these terms introduces a first-order error in the sensitivity analysis.

The equations obeyed by the α -derivatives of the forward and adjoint fluxes in the two states are found by differentiating forward Eqs. (1) or (4) and adjoint Eqs. (5a) or (5b) with respect to α . For state “s” ($s = 1, 2$), this operation gives

$$(\mathbf{L}_s - \lambda_s \mathbf{P}_s) \frac{\partial \Phi_s}{\partial \alpha} = - \left(\frac{\partial \mathbf{L}_s}{\partial \alpha} - \lambda_s \frac{\partial \mathbf{P}_s}{\partial \alpha} \right) \Phi_s + \frac{\partial \lambda_s}{\partial \alpha} \mathbf{P}_s \Phi_s \quad ; \quad (17a)$$

$$(\mathbf{L}_s^* - \lambda_s \mathbf{P}_s^*) \frac{\partial \Phi_s^*}{\partial \alpha} = - \left(\frac{\partial \mathbf{L}_s^*}{\partial \alpha} - \lambda_s \frac{\partial \mathbf{P}_s^*}{\partial \alpha} \right) \Phi_s^* + \frac{\partial \lambda_s}{\partial \alpha} \mathbf{P}_s^* \Phi_s^* . \quad (17b)$$

Equations (17a) and (17b) are not eigenvalue equations, but rather are examples of “generalized” forward and adjoint equations that have a singular operator such as $(\mathbf{L}_1 - \lambda_1 \mathbf{P}_1)$ and an inhomogeneous source term.¹² These types of generalized solutions are the basis of GPT, which is discussed later.

In principle, Eq. (17a) can be solved to obtain the flux derivative, which could then be substituted into Eq. (16) to obtain the sensitivity coefficient. However, this approach usually is inefficient because Eq. (17) must be solved for each data parameter α .

An alternative approach is to judiciously select the floating weight functions appearing in the general sensitivity coefficient expression. The term containing the flux derivative in Eq. (16) will vanish if the arbitrary function $\tilde{\varphi}_1^*$ is defined to be the solution to the adjoint equation in Eq. (4), so that $\tilde{\varphi}_1^* \rightarrow \Phi_1^*$. Substituting Φ_1^* for $\tilde{\varphi}_1^*$ in Eq. (16) produces the conventional expressions for the eigenvalue sensitivity coefficients:

$$S_{\lambda_s, \alpha} = \frac{\left\langle \Phi_s^* \left(\frac{\alpha \partial \mathbf{L}_s}{\partial \alpha} - \lambda_s \frac{\alpha \partial \mathbf{P}_s}{\partial \alpha} \right) \Phi_s \right\rangle}{\lambda_s \langle \Phi_s^* \mathbf{P}_s \Phi_s \rangle} = \frac{\left\langle \Phi_s^* \frac{\alpha \partial \mathbf{L}_s}{\partial \alpha} \Phi_s \right\rangle}{\langle \Phi_s^* \mathbf{L}_s \Phi_s \rangle} - \frac{\left\langle \Phi_s^* \frac{\alpha \partial \mathbf{P}_s}{\partial \alpha} \Phi_s \right\rangle}{\langle \Phi_s^* \mathbf{P}_s \Phi_s \rangle} , \quad (18)$$

where $s=1$ or 2 to designate the state of interest. The notation in Eq. (18) has no tilde on the sensitivity coefficient, since this expression no longer contains any arbitrary weight functions. These expressions are exact and no longer contain any arbitrary functions, but they require the solution of *two* eigenvalue equations (a forward and adjoint) for the state of interest. However, the adjoint eigenvalue equation must be solved only once—a substantial reduction in computation effort compared with solving Eq. (17a) or (17b) for each α . The TSUNAMI calculation sequences in SCALE perform forward and adjoint

eigenvalue calculations in 1D or 3D geometry and then evaluate Eq. (18) to obtain group-dependent sensitivity profiles for each nuclide-reaction pair.

III.B. Reactivity Sensitivity Coefficients for Data Parameters

The relative sensitivity coefficient for the reactivity response $\rho_{1 \rightarrow 2}$ is defined as

$$S_{\rho, \alpha} = \frac{\alpha}{\rho_{1 \rightarrow 2}} \frac{\partial \rho_{1 \rightarrow 2}}{\partial \alpha} . \quad (19)$$

Unlike the eigenvalue response, the reactivity response may be either positive or negative. This can be a source of confusion when interpreting the relative sensitivity coefficient for the reactivity; hence, a useful convention is to use the *absolute value* of $\rho_{1 \rightarrow 2}$ appearing in the denominator of Eq. (19). With this convention, a negative value of $S_{\rho, \alpha}$ means that an increase in the value of α will cause a negative reactivity to become more negative and a positive reactivity to become less positive. In other words, the sign of $S_{\rho, \alpha}$ is determined by the sign of $\Delta \rho_{1 \rightarrow 2}$ resulting from a positive $\Delta \alpha$.

The reactivity sensitivity coefficient is obtained by differentiating either the eigenvalue-difference equation in Eq. (9) or the exact perturbation theory expression in Eq. (12). First, consider the approach based on eigenvalue differences. In this case the reactivity sensitivity coefficient is equal to

$$\tilde{S}_{\rho, \alpha} = \frac{\alpha}{\rho_{1 \rightarrow 2}} \left[\frac{\partial \lambda_1}{\partial \alpha} - \frac{\partial \lambda_2}{\partial \alpha} \right] = \frac{\lambda_1 \tilde{S}_{\lambda_1, \alpha} - \lambda_2 \tilde{S}_{\lambda_2, \alpha}}{\rho_{1 \rightarrow 2}} . \quad (20)$$

Thus the reactivity sensitivity can be calculated directly from the eigenvalue sensitivity coefficients at states 1 and 2, respectively. Again, the tilde on the sensitivity coefficient implies that arbitrary functions may appear in Eq. (20).

Substituting the general expressions for the eigenvalue sensitivity coefficient from Eq. (16) into Eq. (20) gives the general equation for the reactivity sensitivity coefficient:

$$\tilde{S}_{\rho_1, \alpha} = \frac{\alpha}{\rho_{1 \rightarrow 2}} \left\{ \frac{\left\langle \tilde{\varphi}_1^* \left(\frac{\partial \mathbf{L}_1}{\partial \alpha} - \lambda_1 \frac{\partial \mathbf{P}_1}{\partial \alpha} \right) \Phi_1 \right\rangle}{\left\langle \tilde{\varphi}_1^* \mathbf{P}_1 \Phi_1 \right\rangle} - \frac{\left\langle \tilde{\varphi}_2^* \left(\frac{\partial \mathbf{L}_2}{\partial \alpha} - \lambda_2 \frac{\partial \mathbf{P}_2}{\partial \alpha} \right) \Phi_2 \right\rangle}{\left\langle \tilde{\varphi}_2^* \mathbf{P}_2 \Phi_2 \right\rangle} + \frac{\left\langle \frac{\partial \Phi_1}{\partial \alpha} (\mathbf{L}_1^* - \lambda_1 \mathbf{P}_1^*) \tilde{\varphi}_1^* \right\rangle}{\left\langle \tilde{\varphi}_1^* \mathbf{P}_1 \Phi_1 \right\rangle} - \frac{\left\langle \frac{\partial \Phi_2}{\partial \alpha} (\mathbf{L}_2^* - \lambda_2 \mathbf{P}_2^*) \tilde{\varphi}_2^* \right\rangle}{\left\langle \tilde{\varphi}_2^* \mathbf{P}_2 \Phi_2 \right\rangle} \right\}. \quad (21)$$

The same type of derivation can also be done using Eqs. (7a) and (7b) rather than Eqs. (6a) and (6b) to evaluate the eigenvalue derivatives.

Equation (21) shows that the reactivity sensitivity coefficient contains two arbitrary weight functions [$\tilde{\varphi}_1^*$, $\tilde{\varphi}_2^*$] and two eigenvalue solutions [Φ_1 , Φ_2], as well as the flux derivatives for states 1 and 2. As was the case for eigenvalue sensitivities, the terms containing these derivatives can be eliminated by selecting the two arbitrary weight functions appropriately. It is easily shown that a special form of the general reactivity coefficient containing no flux or adjoint derivatives is given by the following equation:

$$S_{\rho, \alpha} = \left\{ \frac{\left\langle \Phi_1^* \left(\frac{\alpha \partial \mathbf{L}_1}{\partial \alpha} - \lambda_1 \frac{\alpha \partial \mathbf{P}_1}{\partial \alpha} \right) \Phi_1 \right\rangle}{\rho_{1 \rightarrow 2} \left\langle \Phi_1^* \mathbf{P}_1 \Phi_1 \right\rangle} - \frac{\left\langle \Phi_2^* \left(\frac{\alpha \partial \mathbf{L}_2}{\partial \alpha} - \lambda_2 \frac{\alpha \partial \mathbf{P}_2}{\partial \alpha} \right) \Phi_2 \right\rangle}{\rho_{1 \rightarrow 2} \left\langle \Phi_2^* \mathbf{P}_2 \Phi_2 \right\rangle} \right\}. \quad (22)$$

Four eigenvalue solutions—a forward and an adjoint at both states 1 and 2—are now required to evaluate the reactivity sensitivity coefficient in Eq. (22) that contains no flux/adjoint derivatives, whereas the eigenvalue sensitivity expressions require only *two*

eigenvalue solutions. This form of the reactivity sensitivity coefficient contains no arbitrary weight functions, so a tilde does not appear on S in Eq. (22). A nice feature of Eq. (22) is that it is easily expressed in terms of eigenvalue sensitivity coefficients for the two states, as shown in Eq. (20). It has also been shown that Eq. (22) can be obtained from EGPT.¹⁵

The preceding development uses the reactivity expression defined in terms of eigenvalue-differences. We now derive the reactivity sensitivity coefficient from the exact perturbation theory expression. The result appears quite different from the previous equations. Taking the derivative of Eq. (12) with respect to α and rearranging gives

$$\begin{aligned}
 \frac{\partial \rho_{1 \rightarrow 2}}{\partial \alpha} = & \rho_{1 \rightarrow 2} \left\{ \frac{\left\langle \Phi_1^* \left(\frac{\partial \Delta \mathbf{L}}{\partial \alpha} - \lambda_1 \frac{\partial \Delta \mathbf{P}}{\partial \alpha} \right) \Phi_2 \right\rangle}{\left\langle \Phi_1^* (\Delta \mathbf{L} - \lambda_1 \Delta \mathbf{P}) \Phi_2 \right\rangle} - \frac{\left\langle \Phi_1^* \frac{\partial \mathbf{P}_2}{\partial \alpha} \Phi_2 \right\rangle}{\left\langle \Phi_1^* \mathbf{P}_2 \Phi_2 \right\rangle} \right\} \\
 & + \rho_{1 \rightarrow 2} \left\{ \frac{\left\langle \frac{\partial \Phi_1^*}{\partial \alpha} (\Delta \mathbf{L} - \lambda_1 \Delta \mathbf{P}) \Phi_2 \right\rangle}{\left\langle \Phi_1^* (\Delta \mathbf{L} - \lambda_1 \Delta \mathbf{P}) \Phi_2 \right\rangle} + \frac{\left\langle \Phi_1^* (\Delta \mathbf{L} - \lambda_1 \Delta \mathbf{P}) \frac{\partial \Phi_2}{\partial \alpha} \right\rangle}{\left\langle \Phi_1^* (\Delta \mathbf{L} - \lambda_1 \Delta \mathbf{P}) \Phi_2 \right\rangle} \right\} \\
 & - \rho_{1 \rightarrow 2} \left\{ \frac{\left\langle \Phi_1^* \mathbf{P}_2 \frac{\partial \Phi_2}{\partial \alpha} \right\rangle}{\left\langle \Phi_1^* \mathbf{P}_2 \Phi_2 \right\rangle} + \frac{\left\langle \frac{\partial \Phi_1^*}{\partial \alpha} \mathbf{P}_2 \Phi_2 \right\rangle}{\left\langle \Phi_1^* \mathbf{P}_2 \Phi_2 \right\rangle} \right\} + \frac{\partial \lambda_1}{\partial \alpha} \frac{\left\langle \Phi_1^* \Delta \mathbf{P} \Phi_2 \right\rangle}{\left\langle \Phi_1^* \mathbf{P}_2 \Phi_2 \right\rangle} . \quad (23)
 \end{aligned}$$

Although Eq. (23) depends only on the two functions Φ_1^* and Φ_2 , it also contains their unknown derivatives; and, unlike Eq. (21), it contains no “free” arbitrary functions that can be used to make these terms vanish. These derivatives could be obtained by solving Eqs. (17a) and (17b) for a specified data parameter α ; i.e.,

$$(\mathbf{L}_2 - \lambda_2 \mathbf{P}_2) \frac{\partial \Phi_2}{\partial \alpha} = - \left(\frac{\partial \mathbf{L}_2}{\partial \alpha} - \lambda_2 \frac{\partial \mathbf{P}_2}{\partial \alpha} \right) \Phi_2 + \frac{\partial \lambda_2}{\partial \alpha} \mathbf{P}_2 \Phi_2 \quad ; \quad (24a)$$

$$(\mathbf{L}_1^* - \lambda_1 \mathbf{P}_1^*) \frac{\partial \Phi_1^*}{\partial \alpha} = - \left(\frac{\partial \mathbf{L}_1^*}{\partial \alpha} - \lambda_1 \frac{\partial \mathbf{P}_1^*}{\partial \alpha} \right) \Phi_1^* + \frac{\partial \lambda_1}{\partial \alpha} \mathbf{P}_1^* \Phi_1^* \quad . \quad (24b)$$

However, as previously mentioned, it is usually not practical to solve the above equations for all α of interest; hence an alternative approach based on GPT is used.¹⁴ GPT introduces the “generalized forward” and “generalized adjoint” functions Γ and Γ^* , respectively, defined over the same domains as Φ and Φ^* . For the exact perturbation theory formulation of the reactivity response in Eq. (12), the generalized functions obey the singular inhomogeneous equations:

$$(\mathbf{L}_1 - \lambda_1 \mathbf{P}_1) \Gamma_1 = \mathbf{Q}_1 \equiv \mathbf{A} \Phi_2 \quad \text{and} \quad (25a)$$

$$(\mathbf{L}_2^* - \lambda_2 \mathbf{P}_2^*) \Gamma_2^* = \mathbf{Q}_2^* \equiv \mathbf{A}^* \Phi_1^* \quad , \quad (25b)$$

where the operator \mathbf{A} is defined as

$$\mathbf{A} \equiv \frac{\Delta \mathbf{L} - \lambda_1 \Delta \mathbf{P}}{\langle \Phi_1^* (\Delta \mathbf{L} - \lambda_1 \Delta \mathbf{P}) \Phi_2 \rangle} - \frac{\mathbf{P}_2}{\langle \Phi_1^* \mathbf{P}_2 \Phi_2 \rangle} \quad . \quad (26)$$

The generalized forward and adjoint equations have several interesting features. Because the operators appearing on the left sides of Eqs. (25a) and (25b) are singular, the generalized source terms \mathbf{Q}_1 and \mathbf{Q}_2^* must be orthogonal to the respective homogeneous solutions (i.e., solutions obtained with source terms equal to zero) in order for the inhomogeneous equation to have a solution.¹² The homogeneous solutions of Eqs. (25a) and (25b), respectively, correspond to the forward and adjoint functions Φ_1 and Φ_2^* , which are the fundamental lambda-eigenfunctions of the transport equations in Eqs. (1) and (5b); therefore, the source conditions required for solutions to exist are

$$\langle \Phi_1^* Q_1 \rangle = \langle \Phi_2 Q_2^* \rangle = 0 .$$

It can be seen that the generalized sources in Eq. (25) obey these existence requirements; however, this does not guarantee *unique* solutions to the inhomogeneous equations. It is easily verified that if the homogeneous solution is multiplied by any constant and added to a particular solution of the inhomogeneous equation, then the result also will be a solution.¹² Thus the general solutions to Eqs. (25a) and (25b) are

$$\Gamma_1 \equiv \hat{\Gamma}_1 + \beta_1 \Phi_1 \quad \text{and} \quad (27a)$$

$$\Gamma_2^* \equiv \hat{\Gamma}_2^* + \beta_2 \Phi_2^* \quad , \quad (27b)$$

where $\hat{\Gamma}_1$ and $\hat{\Gamma}_2^*$ are particular inhomogeneous solutions that contain no fundamental mode and β_1 and β_2 are arbitrary constants. These constants can be determined from auxiliary constraints placed on the generalized forward and adjoint solutions, as will be shown later.

Following the standard approach in perturbation theory, we form the inner product of $\frac{\partial \Phi_1^*}{\partial \alpha}$ with Eq. (25a), and of Γ with Eq. (24b), and subtract to obtain

$$\begin{aligned} \frac{\left\langle \frac{\partial \Phi_1^*}{\partial \alpha} (\Delta \mathbf{L} - \lambda_1 \Delta \mathbf{P}) \Phi_2 \right\rangle}{\langle \Phi_1^* (\Delta \mathbf{L} - \lambda_1 \Delta \mathbf{P}) \Phi_2 \rangle} &= - \left\langle \Gamma_1 \left(\frac{\partial \mathbf{L}_1^*}{\partial \alpha} - \lambda_1 \frac{\partial \mathbf{P}_1^*}{\partial \alpha} \right) \Phi_1^* \right\rangle + \frac{\partial \lambda_1}{\partial \alpha} \langle \Gamma_1 \mathbf{P}_1^* \Phi_1^* \rangle \\ &+ \frac{\left\langle \frac{\partial \Phi_1^*}{\partial \alpha} \mathbf{P}_2 \Phi_2 \right\rangle}{\langle \Phi_1^* \mathbf{P}_2 \Phi_2 \rangle} \end{aligned} \quad (28a)$$

Similarly, taking the inner product of $\frac{\partial \Phi_2}{\partial \alpha}$ with Eq. (25b), and of Γ^* with Eq. (24a), and

then subtracting provides the equation

$$\begin{aligned}
 \frac{\left\langle \frac{\partial \Phi_2}{\partial \alpha} (\Delta \mathbf{L}^* - \lambda_1 \Delta \mathbf{P}^*) \Phi_1^* \right\rangle}{\left\langle \Phi_1^* (\Delta \mathbf{L} - \lambda_1 \Delta \mathbf{P}) \Phi_2 \right\rangle} &= - \left\langle \Gamma_2^* \left(\frac{\partial \mathbf{L}_2}{\partial \alpha} - \lambda_2 \frac{\partial \mathbf{P}_2}{\partial \alpha} \right) \Phi_2 \right\rangle + \frac{\partial \lambda_2}{\partial \alpha} \left\langle \Gamma_2^* \mathbf{P}_2 \Phi_2 \right\rangle \\
 &+ \frac{\left\langle \frac{\partial \Phi_2}{\partial \alpha} \mathbf{P}_2^* \Phi_1^* \right\rangle}{\left\langle \Phi_1^* \mathbf{P}_2 \Phi_2 \right\rangle}. \tag{28b}
 \end{aligned}$$

Substituting Eqs. (28a) and (28b) into Eq. (23) eliminates the forward and adjoint derivatives to give

$$\begin{aligned}
 \frac{\partial \rho_{1 \rightarrow 2}}{\partial \alpha} &= \rho_{1 \rightarrow 2} \left\{ \frac{\left\langle \Phi_1^* \left(\frac{\partial \Delta \mathbf{L}}{\partial \alpha} - \lambda_1 \frac{\partial \Delta \mathbf{P}}{\partial \alpha} \right) \Phi_2 \right\rangle}{\left\langle \Phi_1^* (\Delta \mathbf{L} - \lambda_1 \Delta \mathbf{P}) \Phi_2 \right\rangle} - \frac{\left\langle \Phi_1^* \frac{\partial \mathbf{P}_2}{\partial \alpha} \Phi_2 \right\rangle}{\left\langle \Phi_1^* \mathbf{P}_2 \Phi_2 \right\rangle} \right\} \\
 &- \rho_{1 \rightarrow 2} \left\{ \left\langle \Gamma_1 \left(\frac{\partial \mathbf{L}_1^*}{\partial \alpha} - \lambda_1 \frac{\partial \mathbf{P}_1^*}{\partial \alpha} \right) \Phi_1^* \right\rangle + \left\langle \Gamma_2^* \left(\frac{\partial \mathbf{L}_2}{\partial \alpha} - \lambda_2 \frac{\partial \mathbf{P}_2}{\partial \alpha} \right) \Phi_2 \right\rangle \right\} \\
 &+ \rho_{1 \rightarrow 2} \left\{ \frac{\partial \lambda_2}{\partial \alpha} \left\langle \Gamma_2^* \mathbf{P}_2 \Phi_2 \right\rangle + \frac{\partial \lambda_1}{\partial \alpha} \left(\left\langle \Gamma_1 \mathbf{P}_1^* \Phi_1^* \right\rangle - \frac{\left\langle \Phi_1^* \Delta \mathbf{P} \Phi_2 \right\rangle}{\left\langle \Phi_1^* (\Delta \mathbf{L} - \lambda_1 \Delta \mathbf{P}) \Phi_2 \right\rangle} \right) \right\}. \tag{29}
 \end{aligned}$$

The last bracketed expression in Eq (29) contains the unknown derivatives of the lambda eigenvalues for states 1 and 2. These can be eliminated by defining the homogeneous components of functions Γ and Γ^* appropriately. The $\frac{\partial \lambda_2}{\partial \alpha}$ term will be zero if the coefficient $\left\langle \Gamma_2^* \mathbf{P}_2 \Phi_2 \right\rangle \rightarrow 0$, which implies that the generalized adjoint function contains no fundamental mode harmonic. This is accomplished by defining the parameter β_2 in Eq. (27b) to be zero so that $\Gamma_2^* \rightarrow \hat{\Gamma}_2^*$. To make the term containing $\frac{\partial \lambda_1}{\partial \alpha}$ vanish, it is necessary that the generalized forward function satisfy the constraint condition,

$$\langle \Gamma_1 \mathbf{P}_1^* \Phi_1^* \rangle - \frac{\langle \Phi_1^* \Delta \mathbf{P} \Phi_2 \rangle}{\langle \Phi_1^* (\Delta \mathbf{L} - \lambda_1 \Delta \mathbf{P}) \Phi_2 \rangle} = 0 \quad . \quad (30)$$

Substituting Eq. (27a) into Eq. (30), solving for the parameter β_1 gives

$$\beta_1 = \frac{\langle \Phi_1^* \Delta \mathbf{P} \Phi_2 \rangle}{\langle \Phi_1^* \mathbf{P}_1 \Phi_1 \rangle \langle \Phi_1^* (\Delta \mathbf{L} - \lambda_1 \Delta \mathbf{P}) \Phi_2 \rangle} \quad , \quad (31a)$$

so that

$$\Gamma_1 \equiv \hat{\Gamma}_1 + \left(\frac{\langle \Phi_1^* \Delta \mathbf{P} \Phi_2 \rangle}{\langle \Phi_1^* \mathbf{P}_1 \Phi_1 \rangle \langle \Phi_1^* (\Delta \mathbf{L} - \lambda_1 \Delta \mathbf{P}) \Phi_2 \rangle} \right) \Phi_1 \quad . \quad (31b)$$

If there is no difference in the fission production operators for states 1 and 2 (i.e., $\Delta \mathbf{P} \rightarrow 0$), as often occurs for coolant void reactivity or moderator temperature coefficient responses, then the value of β_1 is zero, and the generalized forward function also contains no fundamental mode harmonic. Otherwise, the fundamental mode component should be included in Γ_1 . The generalized forward and adjoint equations are most easily solved numerically by computing the “uncontaminated” solutions $\hat{\Gamma}_1$ and $\hat{\Gamma}_2^*$ that have no fundamental harmonic. The uncontaminated solutions then are converted to the general solution by adding the amount of fundamental mode shown in Eq. (31b).

Assuming that the generalized forward and adjoint functions are defined as described above, the last bracketed term in Eq. (29) becomes zero. The resulting expression is substituted into Eq. (19) to obtain another exact equation for the reactivity sensitivity coefficient:

$$S_{\rho, \alpha} = \left\{ \frac{\left\langle \Phi_1^* \left(\frac{\alpha \partial \Delta \mathbf{L}}{\partial \alpha} - \lambda_1 \frac{\alpha \partial \Delta \mathbf{P}}{\partial \alpha} \right) \Phi_2 \right\rangle}{\langle \Phi_1^* (\Delta \mathbf{L} - \lambda_1 \Delta \mathbf{P}) \Phi_2 \rangle} - \frac{\left\langle \Phi_1^* \frac{\alpha \partial \mathbf{P}_2}{\partial \alpha} \Phi_2 \right\rangle}{\langle \Phi_1^* \mathbf{P}_2 \Phi_2 \rangle} \right\} \quad \text{direct}$$

$$- \left\{ \left\langle \Gamma_1 \left(\frac{\alpha \partial \mathbf{L}_1^*}{\partial \alpha} - \lambda_1 \frac{\alpha \partial \mathbf{P}_1^*}{\partial \alpha} \right) \Phi_1^* \right\rangle + \left\langle \Gamma_2^* \left(\frac{\alpha \partial \mathbf{L}_2}{\partial \alpha} - \lambda_2 \frac{\alpha \partial \mathbf{P}_2}{\partial \alpha} \right) \Phi_2 \right\rangle \right\}_{indirect} \quad (32)$$

This equation can also be derived from a variational principle.¹⁴

In the parlance of GPT, the first bracketed term in Eq. (32) is called the “direct” effect of the perturbation in α . It corresponds to the partial α -derivative of the response, evaluated at the reference (unperturbed) values of the flux and adjoint functions. Once the reference reactivity has been calculated by solving the forward and adjoint equation at states 1 and 2, respectively, the direct effect is found easily with no additional flux or adjoint solutions. The last bracketed expression in Eq. (32) is the “indirect” effect that accounts for the impact of the α -perturbation on the reference solutions Φ_1^* and Φ_2 . Evaluation of the indirect effect requires additional calculations for the generalized forward and adjoint functions. Several codes have been developed for this purpose.¹²

Because the expressions in Eqs. (32), (22), and (20) must all be equivalent, a relationship can be established between the generalized and the regular forward/adjoint functions. First, the direct term [first bracketed term on the right side of Eq. (32)] is manipulated to obtain

$$\begin{aligned} \left\{ S_{\rho, \alpha} \right\}_{direct} &= \left(\frac{\lambda_1 \tilde{S}_{\lambda_1, \alpha} - \lambda_2 \tilde{S}_{\lambda_2, \alpha}}{\rho_{1 \rightarrow 2}} \right) \\ &- \left\langle \left(\frac{\Phi_2}{\rho \langle \Phi_1^* \mathbf{P}_2 \Phi_2 \rangle} - \frac{\Phi_1}{\rho \langle \Phi_1^* \mathbf{P}_1 \Phi_1 \rangle} \right) \left(\frac{\alpha \partial \mathbf{L}_1^*}{\partial \alpha} - \lambda_1 \frac{\alpha \partial \mathbf{P}_1^*}{\partial \alpha} \right) \Phi_1^* \right\rangle \\ &- \left\langle \left(\frac{\Phi_2^*}{\rho \langle \Phi_2^* \mathbf{P}_2 \Phi_2 \rangle} - \frac{\Phi_1^*}{\rho \langle \Phi_1^* \mathbf{P}_1 \Phi_1 \rangle} \right) \left(\frac{\alpha \partial \mathbf{L}_2}{\partial \alpha} - \lambda_2 \frac{\alpha \partial \mathbf{P}_2}{\partial \alpha} \right) \Phi_2 \right\rangle \quad (33) \end{aligned}$$

From Eq. (20), the first term on the right side is equal to $S_{\rho,\alpha}$; therefore, after substituting

Eq. (33) back into the GPT expression in Eq. (32), the following identities are found:

$$\Gamma = \left(\frac{\Phi_2}{\rho \langle \Phi_1^* \mathbf{P}_2 \Phi_2 \rangle} - \frac{\Phi_1}{\rho \langle \Phi_1^* \mathbf{P}_1 \Phi_1 \rangle} \right); \quad (34a)$$

$$\Gamma^* = \left(\frac{\Phi_2^*}{\rho \langle \Phi_2^* \mathbf{P}_2 \Phi_2 \rangle} - \frac{\Phi_1^*}{\rho \langle \Phi_1^* \mathbf{P}_1 \Phi_1 \rangle} \right). \quad (34b)$$

The above equations show that the generalized functions for reactivity responses are simply related to differences in the appropriately normalized forward and adjoint functions, respectively, of the two states.

In this section, two different expressions have been derived for the reactivity sensitivity coefficient. The first, given by Eq. (20) or (22), is based on the eigenvalue-difference definition of reactivity; and the second, given in Eq. (32), is based on the exact perturbation theory formulation. It is interesting to note that both the GPT and eigenvalue-difference expressions contain four functions that must be calculated. The eigenvalue-difference formulation requires a regular forward and regular adjoint eigenvalue calculation at both system states, while the GPT expression requires a generalized forward and a regular adjoint calculation at state 1, and a regular forward and a generalized adjoint calculation at state 2. Both expressions for the linear sensitivity coefficients have no approximations, so in theory the reactivity perturbation estimated with either formulation is exact through all first-order terms. However, the eigenvalue-difference method has the great advantage of using standard eigenvalue sensitivity coefficients for the two states, so established S/U techniques such as those performed by TSUNAMI can be utilized. The generalized solutions are more difficult to compute and

require additional eigenvalue calculations to treat the fundamental mode components. Furthermore, unlike eigenvalue sensitivity cases where 3D forward and adjoint solutions can be evaluated rather routinely using Monte Carlo codes,¹⁰ no Monte Carlo methods are currently available for computing generalized solutions.

Thus a method based on eigenvalue differences appears to be the better approach for S/U analysis of reactivity associated with two distinct states. However, it has been suggested that the GPT approach could possibly provide more accurate numerical results in some cases because the generalized sources explicitly contain the system change-of-state terms; therefore, the generalized solutions are tightly coupled to the space-dependent perturbations that generate the reactivity.¹⁴ Nevertheless, in this work, reactivity sensitivity coefficients are computed from Eq. (20), which is easily evaluated from conventional eigenvalue sensitivity coefficients at the two states. A computer program has been developed to read the eigenvalue sensitivity profiles computed by TSUNAMI and combine them to obtain group-dependent reactivity sensitivity coefficients by nuclide-reaction pair.

III.C. Implicit Sensitivity Effects

The sensitivity coefficient expressions previously derived describe the effect of varying parameters, such as multigroup cross sections, appearing explicitly in the transport solved for the eigenvalue. In addition to having an explicit impact on the calculated eigenvalue, perturbations in nuclear data or in concentrations of one material may alter the multigroup cross sections of other materials as a result of resonance self-

shielding effects. These indirect variations in the self-shielded cross sections cause additional changes in the eigenvalue, which have been called the “implicit effects” of the original data perturbation.¹⁶ For example, direct perturbations in non-fuel materials such as moderators can implicitly affect the group cross sections of fuel nuclides owing to changes in resonance self-shielding associated with Dancoff effects. It has been shown that implicit changes in the resonance capture cross sections of ^{238}U can be an important component of the overall eigenvalue sensitivity coefficient in thermal systems.¹⁷ Implicit effects are handled by adding an additional term to the usual explicit sensitivity coefficient. The complete eigenvalue sensitivity coefficient, $S_{\lambda}^{(\text{com})}$, is then defined as¹¹

$$S_{\lambda}^{(\text{com})} = S_{\lambda}^{(\text{ex})} + S_{\lambda}^{(\text{im})}$$

where

$S_{\lambda,\alpha}^{(\text{ex})}$ is the explicit eigenvalue sensitivity coefficient given in Eq. (18);

$S_{\lambda,\alpha}^{(\text{im})}$ is the implicit sensitivity coefficient defined as

$$S_{\lambda,\alpha}^{(\text{im})} = \sum_{\alpha'} S_{\lambda,\alpha'}^{(\text{ex})} S_{\alpha',\alpha} ; \text{ and}$$

$S_{\alpha',\alpha}$ is a sensitivity coefficient of multigroup data α' to changes in data α .

For example, $S_{\alpha',\alpha}$ could correspond to the sensitivity of the shielded ^{238}U multigroup cross section to changes in the hydrogen scatter cross section. The TSUNAMI computation sequence calculates the implicit term for eigenvalue sensitivities.¹¹ Thus if the reactivity sensitivity coefficient is determined from Eq. (20) based on eigenvalue differences, the implicit effects are automatically taken into account by TSUNAMI.

V. UNCERTAINTY ANALYSIS FOR EIGENVALUE-DIFFERENCES

One of the common applications of sensitivity coefficients is to determine the uncertainty in responses due to uncertainties in input nuclear data. ORNL has automated this procedure to determine the uncertainty in predicted multiplication factors for criticality safety analysis.¹¹ Uncertainty analysis for a reactivity response can be conducted in a similar manner. The absolute variance (VAR) of an eigenvalue-difference response such as the reactivity $\rho_{1 \rightarrow 2}$ is found from well-known propagation of error expressions to be equal to

$$\text{VAR}(\rho_{1 \rightarrow 2}) \equiv \text{VAR}(\lambda_1 - \lambda_2) = \text{VAR}(\lambda_1) + \text{VAR}(\lambda_2) - 2\text{COV}(\lambda_1, \lambda_2) \quad . \quad (35)$$

The variance in the reactivity is not simply the sum of the variances in the computed eigenvalues for states 1 and 2 if these uncertainties are correlated as a result of using the same nuclear data and models in the transport calculations. The covariance term accounts for the correlation in the two states and may either be a positive or negative effect.

The corresponding *relative* variance of the eigenvalue-difference is equal to

$$\sigma_{\rho}^2 = \left(\frac{\lambda_1}{\lambda_1 - \lambda_2} \right)^2 \sigma_{\lambda_1}^2 + \left(\frac{\lambda_2}{\lambda_1 - \lambda_2} \right)^2 \sigma_{\lambda_2}^2 - \left(\frac{2\lambda_1\lambda_2}{(\lambda_1 - \lambda_2)^2} \right) \sigma_{\lambda_2, \lambda_1} \quad , \quad (36)$$

where

$$\sigma_{\rho}^2 \equiv \frac{\text{VAR}(\rho_{1 \rightarrow 2})}{\rho_{1 \rightarrow 2}^2} = \text{relative variance in the calculated reactivity};$$

$$\sigma_{\lambda_1}^2 \equiv \frac{\text{VAR}(\lambda_1)}{\lambda_1^2} \quad , \quad \sigma_{\lambda_2}^2 \equiv \frac{\text{VAR}(\lambda_2)}{\lambda_2^2} = \text{relative variances of the eigenvalues}; \text{ and}$$

$$\sigma_{\lambda_2, \lambda_1} \equiv \frac{\text{COV}(\lambda_1, \lambda_2)}{\lambda_1 \lambda_2} = \text{relative covariance of the two eigenvalues.}$$

The square roots of the above variances correspond to the respective response standard deviations.

It can be seen from Eq. (36) that the relative variance of the reactivity can be substantially greater than the eigenvalue variances whenever the difference in the eigenvalues of the two states is small because the coefficients of $\sigma_{\lambda_1}^2$ and $\sigma_{\lambda_2}^2$ become large. Since this is usually the case for reactivity changes in a reactor, the relative uncertainties in reactivity responses are inherently large.

To obtain the relationship between the reactivity variance and the nuclear data uncertainties, assume that M different types of nuclear data—such as multigroup cross sections for all nuclide-reaction pairs—are used in calculating the reactivity. We will define the M by M nuclear data uncertainty matrix to be \mathbf{C}_{aa} . This symmetric matrix contains relative variances on the diagonal and relative covariances on the off diagonal. Let \mathbf{S}_p be an M dimensional row vector containing the relative sensitivity coefficients for reactivity, as defined in Eq. (22). The relative variance in the calculated reactivity due to the nuclear data uncertainties can be computed from

$$\sigma_p^2 = \mathbf{S}_p \mathbf{C}_{aa} \mathbf{S}_p^T, \quad (37)$$

where the superscript T indicates a transpose operation.

If we define \mathbf{S}_{λ_1} and \mathbf{S}_{λ_2} to be M dimensional row vectors containing relative sensitivity coefficients for all nuclear data used in computing the eigenvalues of the two states, then from Eq. (20) it is seen that the reactivity sensitivity vector is

$$\mathbf{S}_p = \frac{\lambda_1}{\rho_{1 \rightarrow 2}} \mathbf{S}_{\lambda_1} - \frac{\lambda_2}{\rho_{1 \rightarrow 2}} \mathbf{S}_{\lambda_2}. \quad (38)$$

The uncertainty in the calculated reactivity is found by substituting Eq. (38) into Eq. (37):

$$\sigma_p^2 = \left(\frac{\lambda_1}{\rho_{1 \rightarrow 2}} \right)^2 \mathbf{S}_{\lambda_1} \mathbf{C}_{aa} \mathbf{S}_{\lambda_1}^T + \left(\frac{\lambda_2}{\rho_{1 \rightarrow 2}} \right)^2 \mathbf{S}_{\lambda_2} \mathbf{C}_{aa} \mathbf{S}_{\lambda_2}^T - \left(\frac{2\lambda_1\lambda_2}{\rho_{1 \rightarrow 2}^2} \right) \mathbf{S}_{\lambda_2} \mathbf{C}_{aa} \mathbf{S}_{\lambda_1}^T . \quad (39)$$

Another parameter of interest for S/U analysis of eigenvalue-difference responses is the degree of correlation between the two states. The correlation coefficient is defined so that a value of +1 indicates full correlation in the eigenvalues, 0 indicates no correlation, and -1 indicates anti-correlation between the two states. The correlation coefficient $C_{1,2}$ for the two eigenvalue states is equal to

$$C_{1,2} \equiv \frac{\sigma_{\lambda_1, \lambda_2}}{\sigma_{\lambda_1} \sigma_{\lambda_2}} = \frac{\mathbf{S}_{\lambda_2} \mathbf{C}_{aa} \mathbf{S}_{\lambda_1}^T}{\sqrt{\mathbf{S}_{\lambda_1} \mathbf{C}_{aa} \mathbf{S}_{\lambda_1}^T} \cdot \sqrt{\mathbf{S}_{\lambda_2} \mathbf{C}_{aa} \mathbf{S}_{\lambda_2}^T}} . \quad (40)$$

When this definition is substituted into Eq. (36), it is found that

$$\sigma_p^2 = \left(\frac{\lambda_1 \sigma_{\lambda_1}}{\rho_{1 \rightarrow 2}} \right)^2 + \left(\frac{\lambda_2 \sigma_{\lambda_2}}{\rho_{1 \rightarrow 2}} \right)^2 - 2 C_{1,2} \left(\frac{\lambda_1 \sigma_{\lambda_1}}{\rho_{1 \rightarrow 2}} \right) \left(\frac{\lambda_2 \sigma_{\lambda_2}}{\rho_{1 \rightarrow 2}} \right) . \quad (41)$$

It can be seen from Eq. (41) that a positive correlation ($C_{1,2} > 0$) between the eigenvalue states reduces the uncertainty in the reactivity because common uncertainties tend to cancel from the eigenvalue-difference. On the other hand, negative correlations increase the uncertainty. The correlation coefficient also provides useful information whenever the two distinct states correspond to different benchmark experiments. In this case, the correlation coefficient provides a measure of similarity in the two experiments.⁶

VI. APPLICATION TO COOLANT VOID REACTIVITY

The S/U methodology for eigenvalue-differences was validated for a 1D Wigner-Sitz cylindrical model of an LWR pincell consisting of a 2.1% enriched UO_2 fuel pellet at 900 K, with Zr cladding, and water coolant. State 1 corresponds to unvoided water coolant at 600 K, while state 2 has the water voided to 0.1% of the initial density. All other material concentrations and dimensions are held constant. The response corresponds to the eigenvalue-difference for the two states, as defined in Eq. (8).

The TSUNAMI-1D sequence of SCALE, which is based on deterministic rather than Monte Carlo calculations, was utilized in the validation studies to avoid statistical variations in the perturbation results. This computational sequence (a) performs self-shielding calculations for the unresolved and resolved resonance ranges using modified versions of the BONAMI¹⁸ and NITAWL¹⁹ modules, respectively; (b) executes the 1D discrete ordinates code XSDRNPM²⁰ to compute forward and adjoint flux distributions throughout the model; and (c) evaluates perturbation expressions using the SAMS¹¹ module to obtain energy-dependent sensitivity coefficients—both explicit and implicit—relating the multiplication factor to nuclear data variations of all nuclide-reaction pairs. For each nuclide, the energy-dependent sensitivity profiles are also summed over all energy groups and reaction types to obtain “nuclide sensitivities” relating a change in the nuclide concentration to the change in the multiplication factor. TSUNAMI-1D was executed twice—for the unvoided and voided states, respectively—to generate the k -sensitivity coefficients. Another code reads the eigenvalue sensitivities for the two states

and then evaluates Eq. (20) to obtain ρ -sensitivity coefficients for the eigenvalue-difference.

A series of direct calculations was performed in which the input number densities of ^{235}U and ^{238}U , respectively, were varied by $\pm 2\%$. Table 1 shows the multiplication factors and reactivities obtained for the various perturbations considered. Note that these results reflect the impact of concentration changes throughout the entire calculation sequence, i.e., not just in the discrete ordinates eigenvalue calculations but also in the resolved and unresolved self-shielding procedures. Sensitivity coefficients relating the ^{235}U and ^{238}U concentration changes to the concomitant changes in the eigenvalues and reactivity were computed from Table I results by using a central finite-difference approximation. Although not exact, these “direct” estimates for the nuclide sensitivity coefficients are accurate through the second order and can be assumed to be nearly the correct value.

Table II compares the direct results with the nuclide sensitivities calculated from the eigenvalue and reactivity perturbation expressions. It should be noted that in this table, k -sensitivities rather than λ -sensitivities are specified (these have opposite signs) and that the ρ -sensitivity coefficients are defined relative to the *absolute value* of the reactivity, as discussed in section II.2. The perturbation theory results are provided both with and without including the implicit effects of perturbations in self-shielding. It can be seen that the nuclide sensitivity coefficients for the multiplication factor and reactivity responses agree better with direct calculations whenever the implicit effects are included—especially for the ^{238}U atom density, where the implicit effects reduce the magnitudes of k -sensitivities by 10–13% and of the ρ -sensitivity by 8%. The nuclide

sensitivity coefficients with implicit effects all agree to within 0.1% of the direct calculations. The excellent results obtained for this 1D pincell example provide some confidence that the methodology can be used for realistic cases as well.

As an example of a more complex application, S/U calculations were performed for a modified 3D model of the ACR-700 fresh fuel bundle. The computational model used here has been altered from the actual, proprietary ACR-700 design, but most of the sensitivities should be similar. Figure 1 shows the assumed fuel bundle model, consisting of 43 low-enriched UO_2 fuel pins and water coolant inside a ~ 10 -cm-diameter pressure tube, which is placed within a heavy water moderator. For these calculations, an infinite array of fuel bundles such as the one shown in Fig. 1 is assumed within the moderator, so a full core calculation is not required. This assumption is not required in general because a 3D Monte Carlo code is used for the neutron transport computation.

The response considered in this case corresponds to the coolant void reactivity (CVR) associated with voiding of the water coolant inside the pressure tube. In state 1, the coolant inside the fuel bundle is at the reference full power thermal conditions with no voiding; while the water density in state 2 is approximately 0.1% of the initial density, i.e., 99.9% voided. All other material concentrations and dimensions are held constant.

The TSUNAMI-3D sequence was used for the CVR S/U analysis of the fuel bundle. This computational sequence is identical to the TSUNAMI-1D sequence described previously, except that the transport calculations are performed in 3D geometry with the KENO-Va multigroup Monte Carlo code.²¹ The geometry in Fig. 1, with reflected boundary conditions on the outer surfaces (including top and bottom), is the actual KENO model. A 238-group cross-section library based on ENDF/B-V was used in

the transport calculations. The eigenvalues of the two states were determined from the Monte Carlo calculations to a statistical precision of better than 0.01%. For this assumed model of the ACR-700, the CVR is computed to be -211 pcm, with a precision of ± 10 pcm.

Table III shows a comparison of several nuclide sensitivity coefficients calculated for the CVR and for the multiplication factors of the two states. It can be seen that the ρ -sensitivities are often quite large, much greater than the corresponding k -sensitivities for either the unvoided or voided states. For example, the ρ -sensitivity coefficient for deuterium in the heavy water moderator is about 34.3, indicating that a change of 1% in the moderator density could cause more than a 30% change in the CVR. The other CVR sensitivities in Table III have magnitudes ranging from 2 to 7, whereas eigenvalue sensitivities generally are observed to be less than unity for all types of data. An interesting illustration of the difference between eigenvalue and reactivity sensitivities is seen for the nuclide sensitivity of ^{235}U . The CVR sensitivity to the ^{235}U concentration is about -5.0 , while the k -sensitivity coefficients are positive for both unvoided and voided states, with only a small difference in magnitude (~ 0.24 vs 0.23). This means that if the ^{235}U concentration is uniformly increased in the bundle, the multiplication factors for both states will increase; but the voiding reactivity decreases, because the multiplication factor of the initial state increases more than that of the final state. It is interesting to note that the ρ -sensitivity for ^{235}U , as well as ^{238}U , in this fuel bundle is quite different from that found in the LWR pincell example. Like ^{235}U , the ^1H ρ -sensitivity also is a large negative value (~ -2.4) because an increase of the hydrogen atom density in the unvoided

state causes the initial multiplication factor to increase; but this has little impact on the multiplication factor of the voided state, so the CVR decreases.

Table IV shows the CVR sensitivity coefficients for selected cross section data, integrated over all energy. It is seen that the CVR is very sensitive to several types of cross sections, including ^{235}U capture and fission, ^{238}U capture, ^{164}Dy capture (a burnable absorber material), ^1H elastic and capture, and ^2H elastic. These sensitivities, as well as several others not shown, all have magnitudes greater than unity; therefore, the CVR response depends much more strongly on uncertainties in nuclear data than do the eigenvalue responses.

Figures 2 and 3 show energy-dependent sensitivity profiles of the ^{238}U capture data for the unvoided/voided multiplication factors and for the CVR response, respectively. As expected, the ^{238}U capture sensitivities for the multiplication factors in both unvoided and voided states are negative and especially large in magnitude within groups corresponding to the low-energy ^{238}U s-wave resonances (at 6.6 eV, 21 eV, etc.) and within the thermal energy range. However, the CVR sensitivity to this data is much different since the self-shielding of the ^{238}U capture cross section is significantly greater in the voided versus unvoided states. The CVR sensitivity to the ^{238}U capture data is actually positive in the thermal range and around the peaks of the low-energy resonances, even though the integrated sensitivity for these data has a value of about -8.4 , as shown in Table IV. It was verified that the area under the curve in Fig. 3 is, in fact, negative mainly because of the negative sensitivities in the energy range above 100 eV. The wings of the low-energy ^{238}U resonances also tend to have negative sensitivities for the CVR response.

Figures 4 and 5 compare ^{235}U fission sensitivities for the multiplication factor and CVR responses, respectively. The multiplication factors are mainly sensitive to the thermal energy range of this data, and the k-sensitivities are positive in all groups for both states. As a result of loss of moderation in state 2, the CVR has a large negative sensitivity to the ^{235}U fission data in thermal range, while it has positive sensitivities to the epithermal and fast fission data. Table IV shows that the integrated sensitivity for ^{235}U fission is about -3.6 .

Figures 6 and 7 show the CVR sensitivity to the ^1H and ^2H total cross sections. It can be seen that the CVR has positive sensitivity to the ^1H thermal data because of loss of hydrogen absorption in the voided state, but it has large negative sensitivities within the energy intervals of the ^{238}U resonances where the loss of moderation decreases the resonance escape probability. Table IV shows that the hydrogen elastic and absorption data have integrated sensitivity values of about -17.3 and 15.0 , respectively. Thus the net sensitivity for these two competing effects is about -2.4 , corresponding to the overall nuclide sensitivity given in Table III for the hydrogen concentration. The sensitivity of the CVR response to the deuterium total cross sections is very large and positive in the thermal and epithermal ranges. If voiding of the water coolant increases the temperature of the heavy water moderator, then the resulting decrease in the deuterium number density could provide an additional source of negative reactivity for the CVR.

As discussed in section V, the energy-dependent sensitivity profiles for each nuclide-reaction pair can be combined with nuclear data covariance information to calculate the uncertainty in the response. In this work, we have utilized the library of 44 group covariance data that is distributed with the SCALE system.²² These data were

processed from the evaluated uncertainty information in ENDF/B-V; but, unfortunately, there is no covariance information available in this data set for several materials, including deuterium and dysprosium. Thus the results presented here do not include all contributions to the response uncertainty.

The estimated response uncertainties are given in Table V for the state 1 and 2 multiplication factors and for the CVR. Both eigenvalue responses have uncertainties of about 0.8%, while the relative standard deviation of the reactivity response is nearly 50%. This great difference in magnitudes is due to the fact that eigenvalue-difference responses tend to have much larger sensitivities than eigenvalue responses, so the calculated CVR is affected much more strongly by uncertainties in nuclear data. As discussed in section V, the relative variance in eigenvalue-difference responses tends to be amplified for small reactivities, compared with the relative uncertainties in the associated eigenvalues.

Table VI shows the fractional contributions of some important nuclear data to the overall variance in the CVR response. These values depend on a combination of the data uncertainty and the response sensitivity to the data; e.g., a large data uncertainty may not have much contribution if the computed response is insensitive to the data. Based upon available cross-section covariance data, the largest contribution to the CVR uncertainty is found to be the ^{238}U capture data, followed by H elastic, ^{235}U capture, ^{235}U fission. However, the uncertainty analysis does not include the contribution of the deuterium elastic cross section because no covariance data were available. This could be another important contributor to the response uncertainty, since the CVR has the largest sensitivity to this reaction.

VI. SUMMARY

Sensitivity coefficients for eigenvalue-difference responses, such as the reactivity change between two distinct states, can be derived from either eigenvalue perturbation theory or GPT. Both expressions contain four functions that must be computed from either regular or generalized forward and adjoint equations at the two states. However, calculation of the generalized forward and generalized adjoint functions requires more effort, since additional eigenvalue equations must be solved to obtain the fundamental mode components. Furthermore, the reactivity sensitivity coefficients based on eigenvalue perturbation theory can be easily evaluated using conventional sensitivity analysis techniques such as those implemented in the SCALE code system. This allows utilization of previously developed computation sequences such as TSUNAMI-1D and -3D—based on 1D discrete ordinates and 3D Monte Carlo, respectively—to be applied to eigenvalue-difference responses. Reactivity sensitivities computed by eigenvalue perturbation theory were shown to agree well with direct calculations for an LWR pincell case.

The uncertainty in eigenvalue-difference responses depends upon the variances in the eigenvalues of both states, as well as a covariance term that accounts for correlations in the calculations of the states. The relative uncertainty in a reactivity response may be greatly amplified compared with the eigenvalue uncertainties whenever the reactivity change is small. This results in large uncertainties in the calculated values for many reactivity coefficients.

S/U analysis was performed for the coolant void reactivity response in an ACR fuel bundle. The calculations used Monte Carlo to model a fresh fuel bundle in voided and unvoided states. It was found that many of the calculated data sensitivities for the reactivity response are much greater than the corresponding eigenvalue sensitivities for the two states. Uncertainty analysis gives a relative standard deviation in the coolant void reactivity of about 50%, resulting from uncertainties in nuclear data.

Acknowledgments

The author would like to thank Dr. D. E. Carlson of the U. S. Nuclear Regulatory Commission and Dr. J. C. Gehin from Oak Ridge National Laboratory for their support and interest in this study. The work was supported by the NRC Office of Research.

REFERENCES

1. E. P. WIGNER, *Effects of Small Perturbations on Pile Period*, CP-3048, Manhattan Project Report, 1945.
2. L. N. USACHEV, "Perturbation Theory for the Breeding Ratio and Other Number Ratios Pertaining to Various Reactor Processes," *J. Nucl. Energy, Parts A/B*, **18**, 571, (1964).
3. M. L. WILLIAMS, "Development of Depletion Perturbation Theory for Coupled Neutron/Nuclide Fields," *Nucl. Sci. Eng.*, **70**, 20 (1979).
4. J. H. MARABLE, C. R. WEISBIN, and G. DESAUSSURE, "Uncertainty in the Breeding Ratio of a Large Liquid Metal Fast Breeder Reactor," *Nucl. Sci. Eng.*, **75**, 30 (1980).
5. D. G. CACUCI, "Sensitivity for Non-Linear Systems: Nonlinear Functional Analysis Approach," *J. Math. Phys.*, **22**, 12 (1981).
6. B. L. BROADHEAD, B. T. REARDEN, C. M. HOPPER, J. J. WAGSCHAL, and C. V. PARKS, "Sensitivity- and Uncertainty-Based Criticality Safety Validation Techniques," *Nucl. Sci. Eng.*, **146**, 340 (2004).
7. S. GOLUOGLU, C. M. HOPPER, and B. T. REARDEN, "Extended Interpretation of Sensitivity Data for Benchmark Areas of Applicability," *Trans. Am. Nuc. Soc.*, **88**, 77 (2003).
8. *SCALE: A Modular Code System for Performing Standardized Computer Analyses for Licensing Evaluations*, ORNL/TM-2005/39, Version 5, Vols. I–III, April 2005. (Available from Radiation Safety Information Computational Center at Oak Ridge National Laboratory as CCC-725.)

9. B. T. REARDEN, "TSUNAMI-1D: Control Module for One-Dimensional Cross-Section Sensitivity and Uncertainty Analysis for Criticality," in ref. 8, Vol. I, Book 2, Sect. C8.
10. B. T. REARDEN, "TSUNAMI-3D: Control Module for Three-Dimensional Cross Section Sensitivity and Uncertainty Analysis for Criticality," in ref. 8, Vol. I, Book 2, Sect. C9.
11. B. T. REARDEN, "SAMS: Sensitivity Analysis Module for SCALE," in ref. 8, Vol. II, Book 4, Sect. F22.
12. M. L. WILLIAMS, "Perturbation Theory for Nuclear Reactor Analysis," *CRC Handbook of Nuclear Reactors Calculations*, Vol. III, CRC Press, Inc., Boca Raton, Florida, 1986.
13. A. GANDINI, "A Generalized Perturbation Method for Bilinear Functionals of the Real and Adjoint Neutron Fluxes," *J. Nucl. Energy*, **21**, 755 (1967).
14. W. M. STACY, *Variational Methods in Nuclear Reactor Physics*, Academic Press, Oxford, 1974.
15. A. GANDINI, G. PALMIOTTI, and M. SALVATORES, "Equivalent Generalized Perturbation Theory (EGPT)," *Ann. Nuclear Energy* **13**, 109 (1986)
16. M. L. WILLIAMS, B. L. BROADHEAD, and C. V. PARKS, "Eigenvalue Sensitivity Theory for Resonance Shielded Cross Sections," *Nucl. Sci. Eng.*, **138**, 177 (2001).

17. B. T. REARDEN, M. L. WILLIAMS, and J. E. HORWEDEL, "Advances in TSUNAMI Sensitivity and Uncertainty Analysis Codes Beyond SCALE-5," *Trans. Am. Nucl. Soc.*, **92**, 760-762 (June 2005).
18. N. M. GREENE, "BONAMI: Resonance Self-Shielding by the Bondarenko Method," in ref. 8, Vol. II, Book 1, Sect. F1.
19. N. M. GREENE, "NITAWL-III: Scale System Module for Performing Resonance Self-Shielding and Working Library Production," in ref. 8, Vol. II, Book 1, Sect. F2.
20. N. M. GREENE, "XSDRNPM: A One-Dimensional Discrete Ordinates Code for Transport Analysis," in ref. 8, Vol. II, Book 1, Sect. F3.
21. L. M. PETRIE, N. F. LANDERS, D. F. HOLLENBACH, and B. T. REARDEN, "KENO V.a: An Improved Monte Carlo Criticality Program," in ref. 8, Vol. II, Book 2, Sect. F11.
22. B. T. REARDEN, "Sensitivity Utility Modules," in ref. 8, Vol. III, Sect. M18.

TABLE I.

Nuclide Perturbation Results for LWR Pincell in States 1 and 2

Perturbation	Multiplication Factor, State 1 (k_1)	Multiplication Factor, State 2 (k_2)	Reactivity $\rho_{1 \rightarrow 2}$ ($1/k_1 - 1/k_2$)
Unperturbed*	1.123915	0.539069	-0.96530
+2% ^{235}U	1.127959	0.543633	-0.95292
-2% ^{235}U	1.119746	0.534471	-0.97795
+2% ^{238}U	1.117206	0.535436	-0.97255
-2% ^{238}U	1.130722	0.542825	-0.95782

*Reference number densities: $^{235}\text{U}=4.8839E-4$; $^{238}\text{U}=2.2480E-2$.

TABLE II
Nuclide Sensitivity Coefficients for LWR Pincell

Sensitivity Parameter*	Direct Finite Diff Calc	Perturbation Theory (no implicit)	Perturbation Theory (with implicit)
$S_{k1, {}^{235}\text{U}}$	0.1827	0.1832	0.1826
$S_{k2, {}^{235}\text{U}}$	0.4249	0.4259	0.4249
$S_{\rho, {}^{235}\text{U}}$	0.6482	0.6509	0.6482
$S_{k1, {}^{238}\text{U}}$	-0.3006	-0.3408	-0.3006
$S_{k2, {}^{238}\text{U}}$	-0.3426	-0.3782	-0.3423
$S_{\rho, {}^{238}\text{U}}$	-0.3813	-0.4129	-0.3809

* $S_k \equiv -S_{\lambda}$ = sensitivity of multiplication factor response to atom density changes.
 S_{ρ} = sensitivity of reactivity response to atom density changes.

Table III.
Nuclide Sensitivity Coefficients for ACR Fuel Bundle

Nuclide	S_{k1}^*	S_{k2}^*	S_p^*
U-235	0.245 ($\pm 5.73E-6$)	0.231 ($\pm 4.73E-6$)	-5.015 ($\pm 1.70E-2$)
U-238	-0.209 ($\pm 2.48E-6$)	-0.228 ($\pm 3.52E-6$)	-7.519 ($\pm 1.55E-2$)
H-1	6.268E-03 ($\pm 2.48E-6$)	-1.782E-05 ($\pm 6.45E-9$)	-2.375 ($\pm 9.86E-4$)
H-2	0.0999 ($\pm 2.11E-6$)	0.190 ($\pm 3.43E-6$)	34.317 ($\pm 1.08E-2$)
Dy-164	-0.0145 ($\pm 4.91E-7$)	-0.0215 ($\pm 6.84E-7$)	-2.662 ($\pm 1.33E-3$)

* $S_k \equiv -S_\lambda$ = sensitivity of multiplication factor response to atom density changes.
 S_p = sensitivity of CVR response to atom density changes.

Table IV
Integrated Cross Section Sensitivity Coefficients for CVR

Nuclide	$S_{p,\alpha}^*$ $\alpha = \text{elastic}$	$S_{p,\alpha}^*$ $\alpha = \text{capture}$	$S_{p,\alpha}^*$ $\alpha = \text{fission}$
^{235}U	-0.0315 ($\pm 8.09E-06$)	-1.386 ($\pm 8.39E-03$)	-3.590 ($\pm 2.54E-02$)
^{238}U	-0.628 ($\pm 5.22E-04$)	-8.387 ($\pm 1.76E-02$)	1.649 ($\pm 1.88E-03$)
^1H	-17.287 ($\pm 2.39E-03$)	14.915 ($\pm 2.04E-03$)	0.0
^2H	34.159 ($\pm 1.08E-02$)	0.0437 ($\pm 1.05E-04$)	0.0
Dy-164	-0.0151 ($\pm 3.85E-06$)	-2.647 ($\pm 1.33E-03$)	0.0

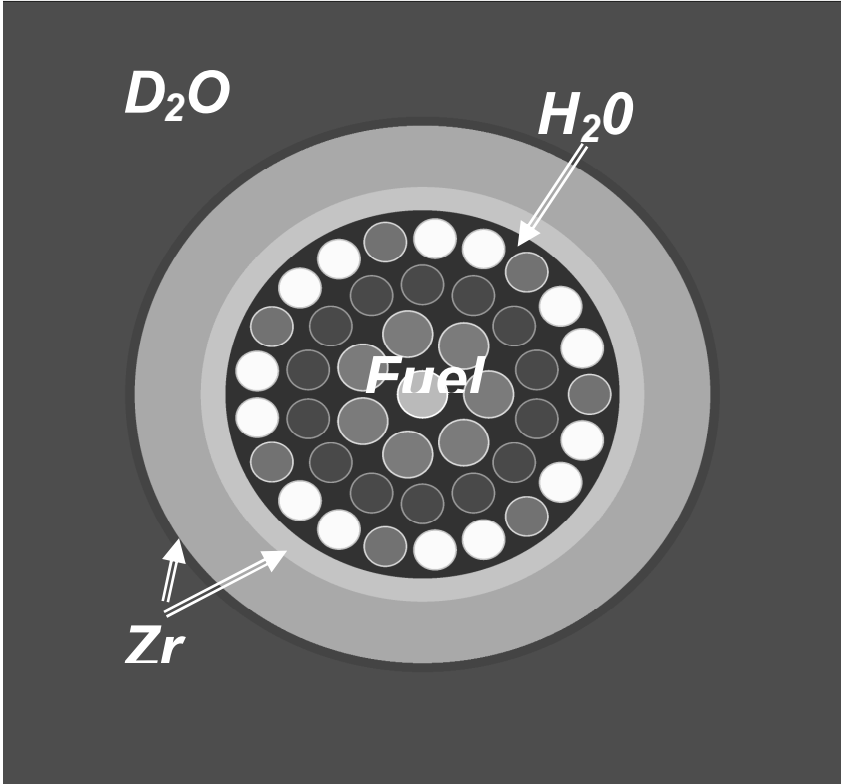
* S_p = sensitivity of CVR response to indicated nuclear data.

Table V
Response Uncertainties Due to Available Nuclear Data Covariances

Response	Relative Standard Deviation (%)
Multiplication factor for state 1	0.80
Multiplication factor for state 2	0.84
Coolant void reactivity (CVR)	49.8

Table VI
Major Data Contributors to CVR Uncertainty

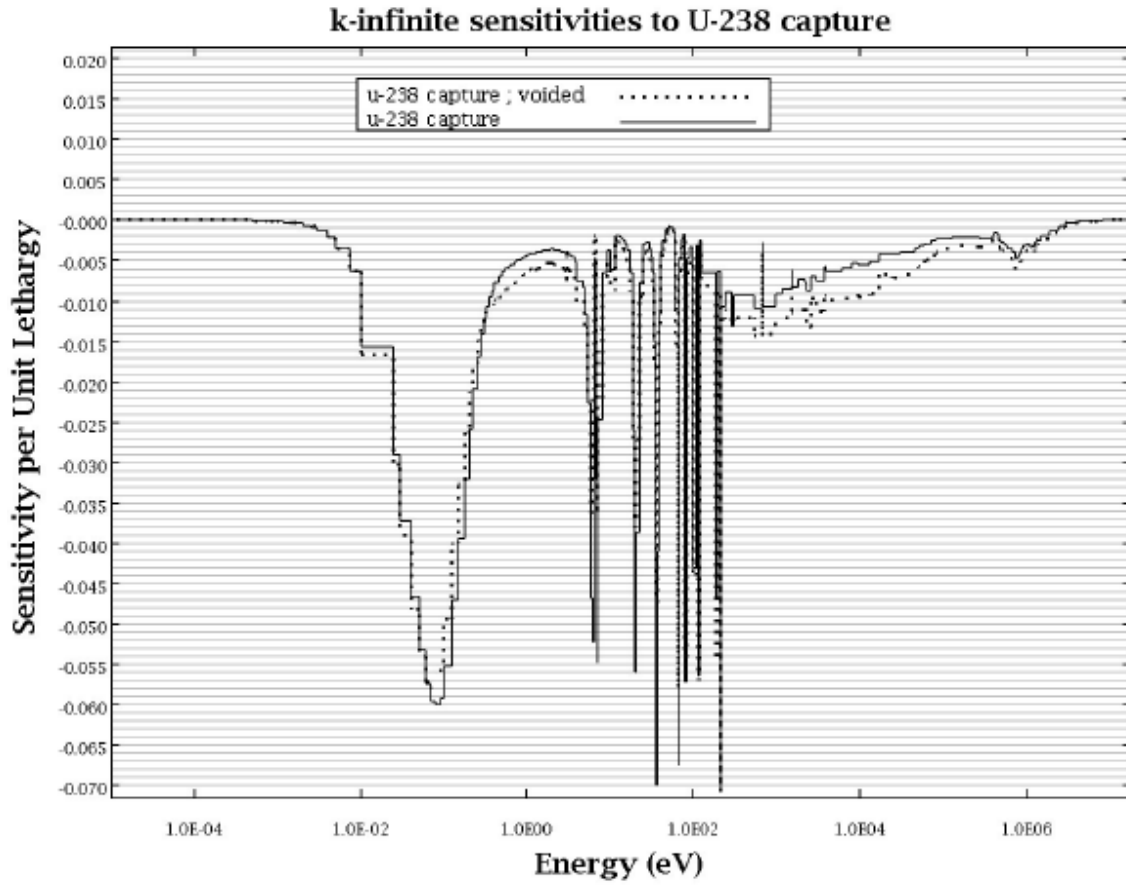
Data	% Contribution to Reactivity Variance
^{238}U n, gamma	4.55E+01
^1H elastic	1.94E+01
^{235}U n, gamma	1.86E+01
^{235}U fission	8.15E+00
^{235}U nubar	3.85E+00
^1H n, gamma	3.23E+00
^{238}U fission	4.88E-01
^{238}U n,n'	3.55E-01
^{238}U nubar	2.41E-01
^{235}U chi	1.31E-01



Sensitivity and Uncertainty Analysis for Eigenvalue-Difference Responses

Mark L. Williams

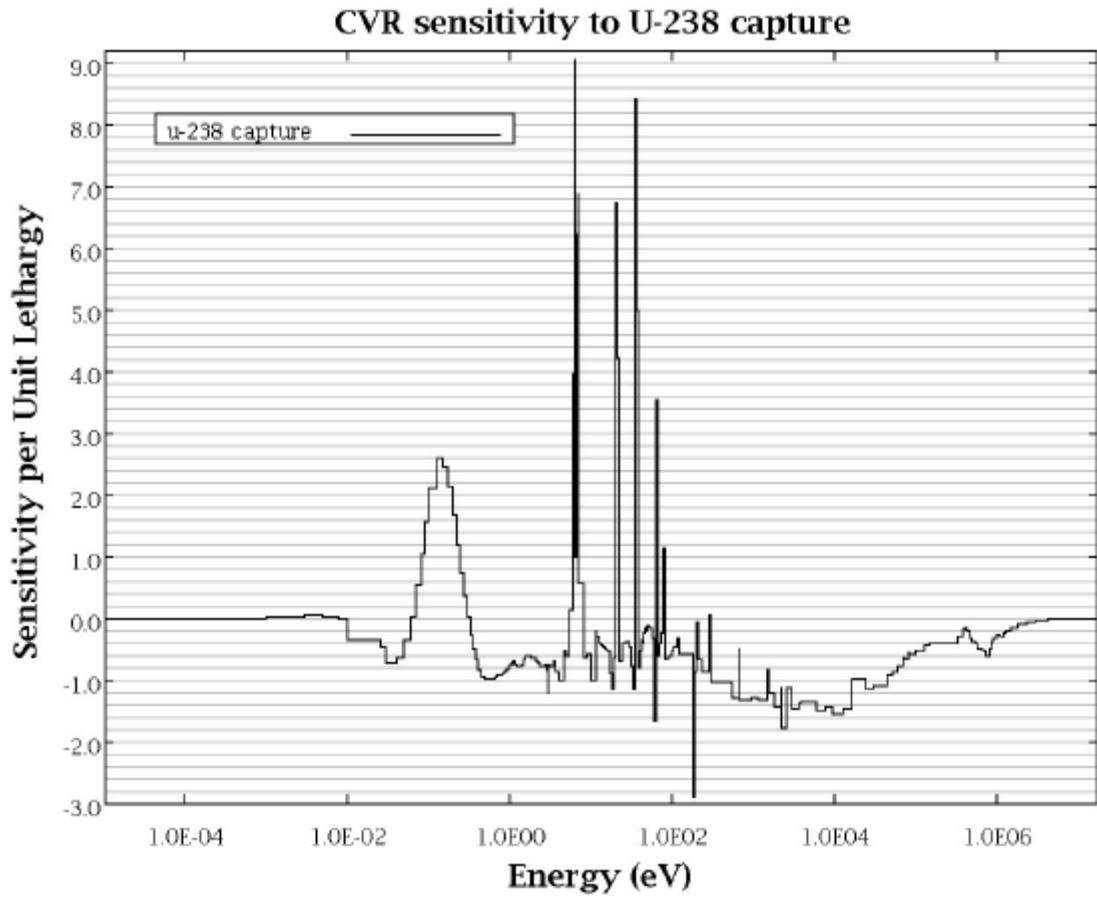
Fig. 1. Modified model for fuel bundle of advanced CANDU reactor.



Sensitivity and Uncertainty Analysis for Eigenvalue-Difference Responses

Mark L. Williams

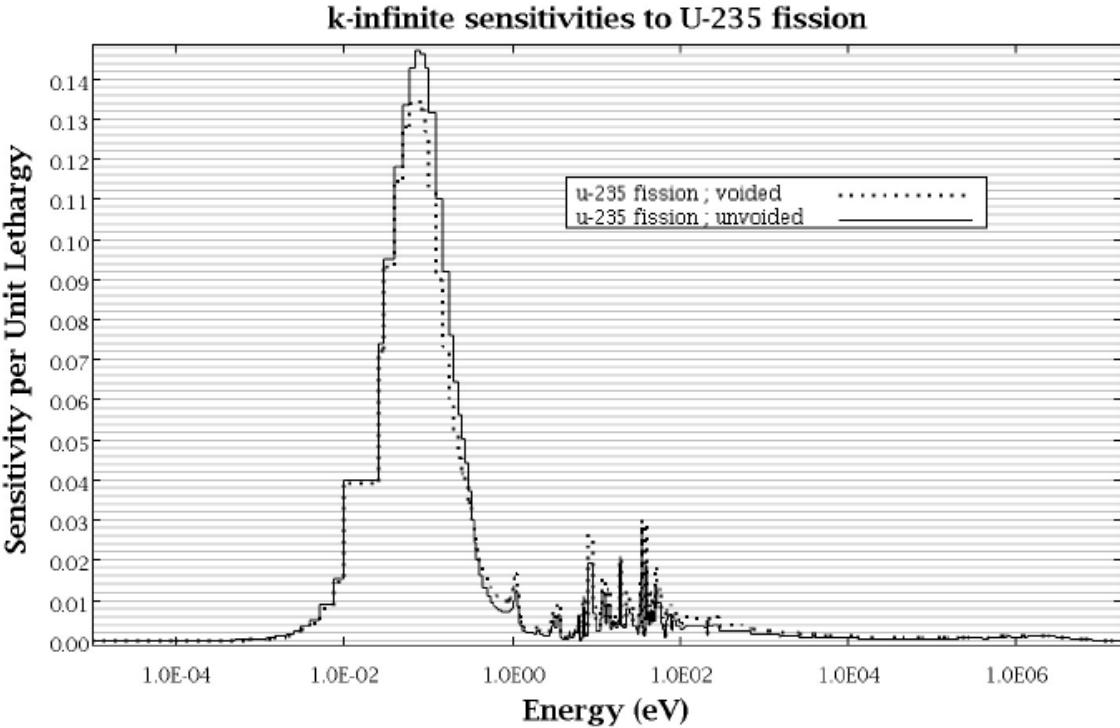
Fig. 2. ^{238}U Capture Sensitivity Profiles for Multiplication Factors in Unvoided and Voided Fuel Bundle



Sensitivity and Uncertainty Analysis for Eigenvalue-Difference Responses

Mark L. Williams

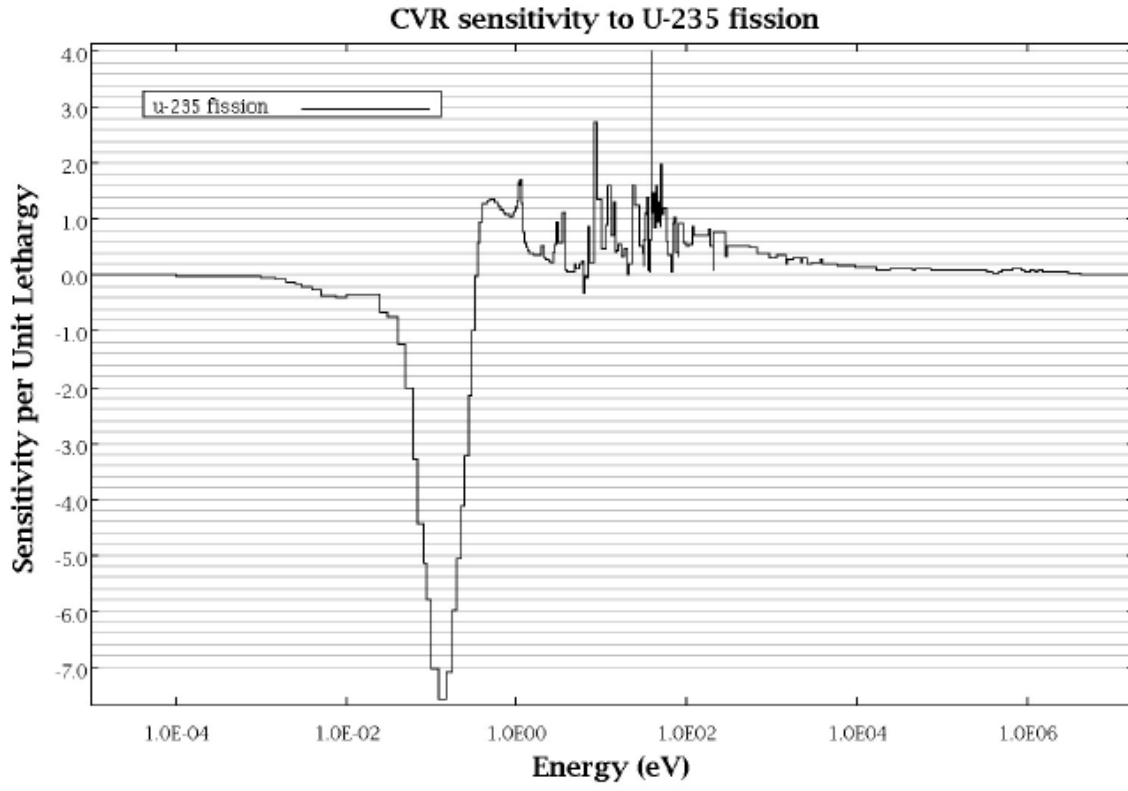
Fig. 3. ^{238}U Capture Sensitivity Profiles for CVR



Sensitivity and Uncertainty Analysis for Eigenvalue-Difference Responses

Mark L. Williams

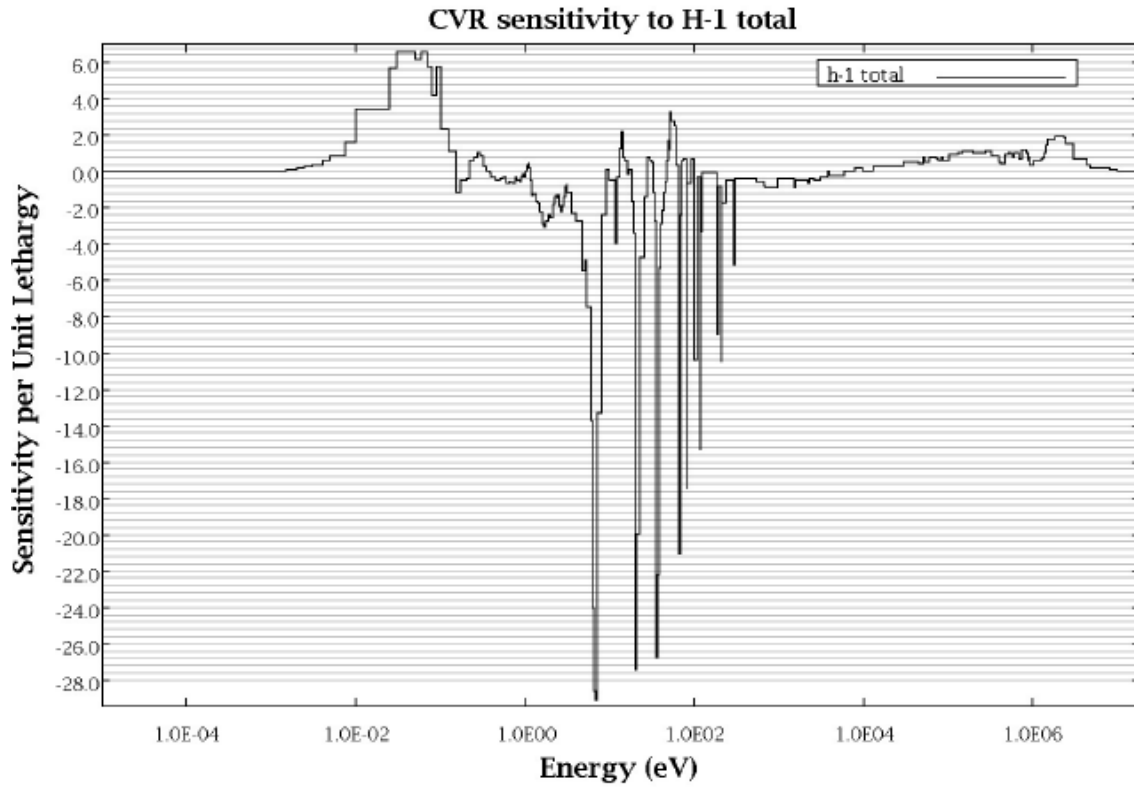
Fig. 4. ^{235}U Fission Sensitivity Profiles for Multiplication Factors
in Unvoided and Voided Fuel Bundle



Sensitivity and Uncertainty Analysis for Eigenvalue-Difference Responses

Mark L. Williams

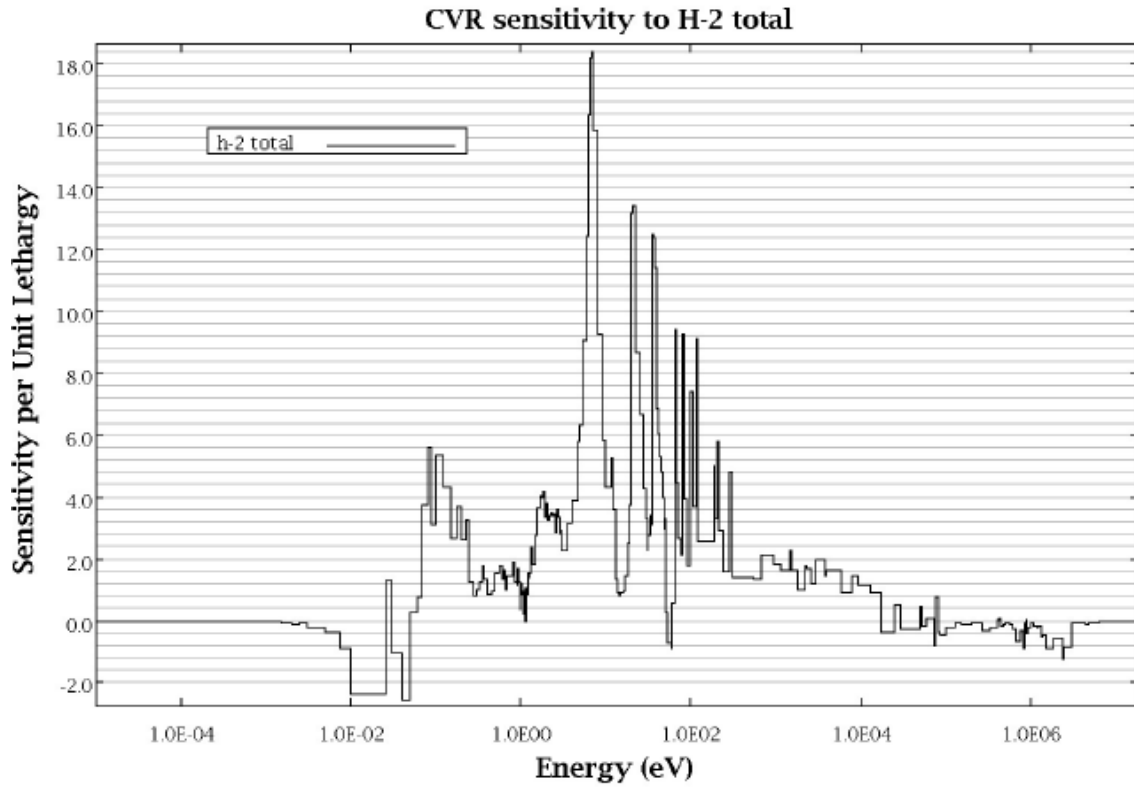
Fig. 5. ^{235}U Fission Sensitivity Profiles for CVR



Sensitivity and Uncertainty Analysis for Eigenvalue-Difference Responses

Mark L. Williams

Fig. 6. Hydrogen Total Cross Section Sensitivity Profiles for CVR



Sensitivity and Uncertainty Analysis for Eigenvalue-Difference Responses

Mark L. Williams

Fig. 7. Deuterium Total Cross Section Sensitivity Profiles for CVR

FIGURE CAPTIONS

Fig. 1. Modified model for fuel bundle of advanced CANDU reactor.

Fig. 2. ^{238}U capture sensitivity profiles for multiplication factors in unvoided and voided fuel bundle.

Fig. 3. ^{238}U capture sensitivity profiles for CVR.

Fig. 4. ^{235}U fission sensitivity profiles for multiplication factors in unvoided and voided fuel bundle.

Fig. 5. ^{235}U fission sensitivity profiles for CVR.

Fig. 6. Hydrogen total cross-section sensitivity profiles for CVR.

Fig. 7. Deuterium total cross-section sensitivity profiles for CVR.